

1/1

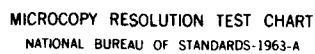
1/1

F/G 17/1

NL

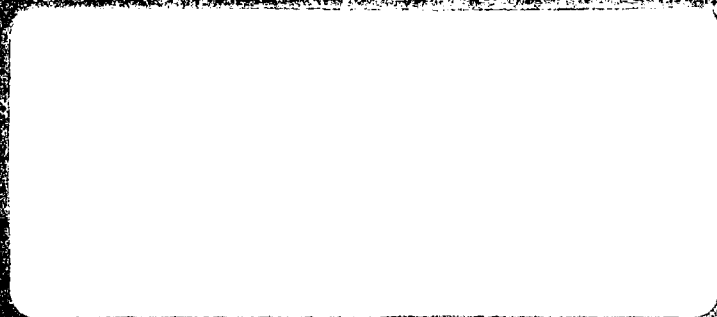
END  
DATE  
FILMED  
6-84  
DTIC





MICROCOPY RESOLUTION TEST CHART  
NATIONAL BUREAU OF STANDARDS-1963-A

AD-A140 922



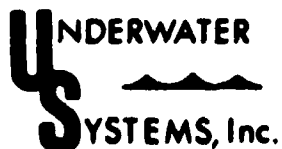
ALGORITHMIC DESIGN OF A CLASSIFICATION  
SYSTEM FOR AT-SEA NUCLEAR DETONATIONS

Prepared For:  
Office of Naval Research

Prepared By:  
David F. Young  
Jim B. McQuitty  
Marvin S. Weinstein

Contract N00014-83-C-0762

3 April 1984

 **UNDERWATER**  
**SYSTEMS, Inc.**

1776 East Jefferson St. • Rockville, Md. 20852 • (301) 770-9190

DTIC  
ELECTE  
MAY 9 1984  
A

This document has been approved  
for public release and sale; its  
distribution is unlimited.

UNCLASSIFIED

SECURITY CLASSIFICATION OF THIS PAGE (When Data Entered)

REPORT DOCUMENTATION PAGE		READ INSTRUCTIONS BEFORE COMPLETING FORM
1. REPORT NUMBER	2. GOVT ACCESSION NO.	3. RECIPIENT'S CATALOG NUMBER
	AD-A140922	
4. TITLE (and Subtitle) Algorithmic Design of a Classification System for At-Sea Nuclear Detonations		5. TYPE OF REPORT & PERIOD COVERED FINAL
		6. PERFORMING ORG. REPORT NUMBER
7. AUTHOR(s) David F. Young, Jim B. McQuitty, Marvin S. Weinstein		8. CONTRACT OR GRANT NUMBER(s) N00014-83-C-0762
9. PERFORMING ORGANIZATION NAME AND ADDRESS Underwater Systems, Inc. 1776 E. Jefferson St. Rockville, MD 20852		10. PROGRAM ELEMENT, PROJECT, TASK AREA & WORK UNIT NUMBERS
11. CONTROLLING OFFICE NAME AND ADDRESS Office of Naval Research Department of the Navy Arlington, Virginia 22217		12. REPORT DATE 3 April 1984
		13. NUMBER OF PAGES 67
14. MONITORING AGENCY NAME & ADDRESS (if different from Controlling Office)		15. SECURITY CLASS. (of this report) UNCLASSIFIED
		15a. DECLASSIFICATION/DOWNGRADING SCHEDULE
16. DISTRIBUTION STATEMENT (of this Report)  UNLIMITED		
17. DISTRIBUTION STATEMENT (of the abstract entered in Block 20, if different from Report)  UNLIMITED		
18. SUPPLEMENTARY NOTES		
19. KEY WORDS (Continue on reverse side if necessary and identify by block number) Nuclear Detonation                      Detonation Classification Hydroacoustic Signal                    Atmospheric Detonation Nuclear Monitoring System              Underwater Detonation Nuclear Detection                        Near-Surface Detonation Detonation Localization		
20. ABSTRACT (Continue on reverse side if necessary and identify by block number) An algorithmic design of a system for the hydroacoustic detection, localization and classification of a suspected at-sea nuclear detonation is presented. Based on basic acoustic principles and nuclear blast theory, the system provides an estimate of the yield-vs-depth/altitude curve for a remote suspect event based on the hydroacoustic signal received at a deep-ocean hydrophone. This system can provide a high-confidence determination of whether or not a suspect atmospheric event is nuclear in origin. A lower level of confidence is placed on the determination of the yield-vs-altitude curve for such an event. The (OVER)		

DD FORM 1 JAN 73 1473 EDITION OF 1 NOV 65 IS OBSOLETE

UNCLASSIFIED

SECURITY CLASSIFICATION OF THIS PAGE (When Data Entered)

## Block 20. Abstract

cumulative effect of error in signal measurement, error in acoustic predictions required by the system, and possible inherent inaccuracies in the method used in determining yield vs altitude could result in order-of-magnitude error in yield/altitude determinations. Nevertheless, its implementation would provide a valuable adjunct to the present nuclear monitoring system.

UNCLASSIFIED

SECURITY CLASSIFICATION OF THIS PAGE(When Data Entered)

## FOREWARD

→ This document presents an algorithmic design of a system for the hydroacoustic detection, localization and classification of a suspected at-sea nuclear detonation. Based on basic acoustic principles and nuclear blast theory, the system provides an estimate of the yield-vs-depth/altitude curve for a remote suspect event based on the hydroacoustic signal received at a deep-ocean hydrophone. It is the conclusion of the authors that this system can provide a high-confidence determination of whether or not a suspect atmospheric event is nuclear in origin. A much lower level of confidence is placed on the determination of the yield-vs-altitude curve for such an event. The cumulative effect of error in signal measurement, error in acoustic predictions required by the system, and possible inherent inaccuracies in the method used in determining yield vs altitude could result in order-of-magnitude error in yield/altitude determinations. Nevertheless, its implementation would provide a valuable adjunct to the present nuclear monitoring system.

In addition to the development of system-specific software, implementation of the classification program will require extant propagation loss models, environmental data banks and localization algorithms, all of which currently reside at the Naval Ocean Research and Development Activity (NORDA). It is recommended that the system be implemented on the NORDA computer and that NORDA be designated the responsible activity for its operation.





## Table of Contents

	<u>Page</u>
1. INTRODUCTION. . . . .	1
1.1 Background . . . . .	1
1.2 Hydroacoustic Sensor System. . . . .	3
1.3 Report Organization. . . . .	4
2. COMPUTATIONAL SCHEME. . . . .	6
2.1 Determination of Yield Vs Depth/Altitude . . . . .	6
2.1.1 Yield Vs Depth - Underwater Case. . . . .	8
2.1.2 Yield Vs Altitude - Atmospheric Case. . . . .	10
2.1.3 Yield Vs Depth/Altitude - Near-Surface Case . . . . .	26
2.1.3.1 Above-Surface Region . . . . .	26
2.1.3.2 Below-Surface Region . . . . .	35
2.2 Signal Processing. . . . .	35
2.3 Error Analysis . . . . .	41
3. SUMMARY . . . . .	45
4. RECOMMENDATIONS . . . . .	48
APPENDIX A - DETONATION LOCALIZATION. . . . .	50
A.1 Background . . . . .	50
A.2 Source Location Determination. . . . .	50
A.3 Reverberation Models . . . . .	54
A.3.1 NSWC Reverberation Model. . . . .	55
A.3.2 USI Reverberation Model . . . . .	58
APPENDIX B - SEISMIC SIGNALS. . . . .	62
References. . . . .	67

## List of Figures

<u>Figure No.</u>		<u>Page</u>
1	Ray Acoustics Paths of Interest. . . . .	12
2	The Sound Velocity Profile for the Standard Ocean. . . . .	14
3	Relative Received Level (RRL) Versus Altitude for a 1-Kiloton Detonation - Atmospheric Region - Standard Ocean. . . . .	16
4	Relative Received level (RRL) Versus Altitude for Every Fifth Yield in Yield Family - Atmospheric Region - Standard Ocean . . . . .	17
5	Diagram Illustrating the Relationship Between the Spherical Spreading-to-Cylindrical Spreading Transition Range ( $R_0$ ), the Water Depth ( $d$ ) and the Maximum Inclination Angle at the Source ( $\theta$ ) Associated With the Long-Range Propagation Modes. . . . .	20
6	Normalized Relative Received Level (NRRL) Versus Altitude for Every Fifth Yield in Yield Family - Atmospheric Region - Standard Ocean . . . . .	24
7	Yield Versus Altitude for a 0.02 lb Charge on Axis - Atmospheric Region - Standard Ocean. . . . .	25
8	Relative Received Level (RRL) Versus Altitude for a 1-Kiloton Detonation - Near-Surface Region . . . . .	30
9	Relative Received Level (RRL) Versus Altitude for Every Fifth Yield in Yield Family - Near-Surface Region. . . . .	31
10	Normalized Relative Received Level (NRRL) Versus Altitude for Every Fifth Yield in Yield Family - Near-Surface Region . . . . .	33
11	Yield Versus Altitude for Indicated On-Axis Yields - Near-Surface and Atmospheric Regions - Standard Ocean. . . .	34
A-1	100 Hz Reverberation for a Hypothetical 1-Megaton Detonation in the North Pacific Ocean. . . . .	52
A-2	Geometry Associated with Reverberant Return from a Basin Reflector ("Hot Spot") . . . . .	53
A-3	Simple Basin Model Showing Various Types of Paths from the Source. . . . .	57

## List of Figures (Cont'd.)

<u>Figure No.</u>		<u>Page</u>
A-4	Geometry for the Sea-Surface Reverberation Calculation as Viewed from Above the Surface. . . . .	59
A-5	Coastal Reverberation Model - Upslope Propagation. . . . .	61
B-1	Energy Loss Through the Air-Water Interface as a Function of Altitude for the Indicated Yields . . . . .	64
B-2	Yield/Altitude Curves (Solid Lines) for Indicated Total Excitation Losses. . . . .	66

## List of Tables

<u>Table No.</u>		<u>Page</u>
1	Directly Induced Shock Wave Energy as a Function of Scaled Detonation Altitude . . . . .	28

## 1. INTRODUCTION

### 1.1 Background

Nations which have signed the Partial Test Ban Treaty have agreed not to conduct nuclear weapons tests in the atmosphere, underwater or in space. Nations which have signed the Nuclear Non-proliferation Treaty have agreed not to develop nuclear weapons or assist others to do so.

Monitoring the environment to detect nuclear weapons tests is of interest for several reasons. It is desirable to assure that there is no violation of the Partial Test Ban Treaty or Non-proliferation Treaty by signature nations, and that non-signature nations have not developed nuclear devices.

The technical data on which monitoring systems are based has been obtained over a research period of four decades. The data has been obtained from nuclear tests performed prior to the inception of the various applicable treaties, from legal nuclear tests, from nuclear tests performed in banned environments by nations which have not signed the applicable treaties, from simulation tests performed with chemical high explosives, and from theoretical investigations of the nuclear explosion processes.

The technical basis for detection of nuclear detonations in the banned environments using remote sensors is well established. In addition to the generation of radioactive debris, a nuclear detonation in the atmosphere is characterized by a double light flash and radiation which affects the ionosphere. For an underwater detonation, high level acoustic signals are generated and the efficiency of seismic wave production is very high. The technical problems of monitoring, if any, stem from implementation to obtain sufficient information in a timely fashion.

It has been suggested that we can be certain that a nuclear event has occurred only if radioactive debris is found at the location predicted on the basis of other observations. This is a rather rigid requirement which may be difficult to satisfy. If the event occurs in a remote oceanic region under circumstances where there is no radioactive debris deposited on land, the time delay between the initial observation and the arrival at the scene of vehicles equipped with proper scientific equipment may preclude the acquisition of debris prior to its natural dispersal.

Without comment as to its wisdom or reasonableness, we adopt the view that a viable monitoring system must provide a capability for satisfying the requirement for retrieval of radioactive debris. The total system capability can then be broken down into three broad categories:

- a. A remote sensor system capable of monitoring the known environmental effects with real-time detection and localization of suspect events.
- b. A signal processing system capable of analyzing the data obtained for the suspect event, confirming the detection, improving the localization, and estimating the yield and other pertinent detonation parameters.
- c. A capability for rapid deployment of an appropriate vehicle to the detonation site for retrieval of radioactive debris.

In this study, we will assume that the first of these system categories - the sensor system - is operable. The extent to which appropriate vehicles for retrieval of radioactive debris are maintained is part of a more general overall readiness problem and will not be addressed here. We will consider the second category restricted to underwater or over-ocean atmospheric detonations and the requirements this may impose on the sensor systems.

## 1.2 Hydroacoustic Sensor System

We assume that a total monitoring system has already been deployed which includes the following components and/or capabilities:

- a. Hydrophones are located in each ocean basin of interest to detect the hydroacoustic signals generated by underwater or above-water detonations, and possible T-phase-like signals generated by underground detonations located near a coast.
- b. A seismometer network for detecting the seismic signals generated by underground or underwater detonations.
- c. A satellite system for detecting the double light blip generated by an atmospheric detonation.

It is further assumed that appropriate elements of the system are monitored in real time to detect and identify suspect events. When a suspect event is identified, the hydrophone output recordings would be carefully examined. If direct arrivals are received at three hydrophone locations, the geographical position of the detonation can be determined. If direct arrivals are not observed on three hydrophones, other supporting information is necessary. For an atmospheric detonation, this could be the detonation time based on the satellite observation of the time of occurrence of the double light blip. In any event, we assume that procedures for determining the geographical location of the detonation based on triangulation using direct arrival times and supplementary information have already been implemented.

It is perhaps more realistic to recognize that direct signals will rarely be received on three hydrophones. This is due to a combination of factors. First, the ocean area which has to be monitored is very large while the number of hydrophones employed is necessarily limited. Second, a nation which wishes to evade detection in performing a test with an underwater or above-water

detonation can take advantage of topographic shielding to greatly reduce the probability that a direct signal will be received, even if it does not know where the monitoring hydrophones are located. However, it is much more difficult to select a detonation location for which basin reverberation is not received. It has been found that the reverberation received on a single hydrophone is, in principle, sufficient to permit the application of triangulation principles to determine the geographical location of the source. The techniques for doing this are in the very early stages of development. Nevertheless, the use of reverberation as a means for determining the location of the detonation, and estimating the yield and depth/altitude, is a procedure which should be considered as an addition to the total system capability. However, the major thrust of this study is the definition of procedures for determining the yield and depth/altitude of the detonation from an analysis of the direct arrival observed on a hydrophone once the geographical location of the detonation is known, without our specifying how the location is determined.

### 1.3 Report Organization

Chapter 2 is divided into three major sections. The first section presents the computational scheme for determination of yield vs depth/altitude for a suspect underwater detonation given that an underwater acoustic signal has been received and appropriately processed, and that the location of the suspect event is known. The second section is a discussion of the method to be employed for processing of the received underwater acoustic signal. The final section identifies potential sources of error in the determination of yield vs depth/altitude and provides a brief quantitative analysis based on assumed error statistics.

Chapter 3 provides a brief summary of the procedures and discuss presented in Chapter 2.

Chapter 4 presents the authors' recommendations resulting from t  
l effort.

Appendix A provides a discussion of the methodology to be employ  
determination of the geographic location of a detonation based on the  
pressure-time history of the shot-generated reverberation received at  
hydrophone. Also included are brief descriptions of two extant comp  
implemented reverberation time-history models.

Appendix B presents a brief discussion of the detectability of s  
signals generated by over-water nuclear detonations. A method for re  
the seismic energy generated by deep underwater and atmospheric detor  
provided.



## 2. COMPUTATIONAL SCHEME

Conceptually, the software system for the determination of the yield and depth/altitude of a nuclear event can be divided into two parts. One part comprises those algorithms which are employed to determine a yield-vs-depth/altitude curve for such an occurrence based on the received hydroacoustic signal. The determination of this functional relationship is the heart of the classification (yield and depth/altitude) process and is given major emphasis in this study. Its determination involves the application of nuclear blast theory and basic acoustic principles. The other part of the system comprises those algorithms employed to determine where the event lies on the previously determined yield-vs-depth/altitude curve. This part of the process brings to bear the capabilities of the total monitoring system in providing clues as to the nature of an explosive event. Determinations based on the information provided by the overall system will be quasi-analytical, will necessarily involve a certain degree of subjectivity and, in all likelihood, will never be sufficient to pinpoint an event on the yield-vs-depth/altitude curve. The best that can be hoped for are specifications of yield and depth/altitude within such bounds as to be significantly useful to those at the decision making levels of government.

### 2.1 Determination of Yield Vs Depth/Altitude

The following discussion is prefaced by these basic assumptions. First, it is assumed that the geographic location of the detonation has been determined. Secondly, the hydrophone is assumed to be located within the deep sound channel in water of sufficient depth to support deep RSR propagation. Thirdly, it is assumed that there is no intervening land mass along the great

circle path between the detonation site and the hydroacoustic sensor, precluding reception of a direct signal. And, finally, the distance between the detonation site and the receiver is assumed to be sufficiently great that the geometric spreading of the acoustic energy at the separation distance is essentially cylindrical. It is important to note that the system places no restriction on the propagation conditions at the detonation site. That is, the water column in the vicinity of the site may or may not support RRR or RSR propagation.

Theoretical considerations based on nuclear detonation phenomenology dictate that, from a computational standpoint, we divide the depth/altitude axis into three regions - underwater, atmospheric and near-surface. For a given detonation yield, the underwater region refers to depths greater than  $21W^{1/3}$  feet, where  $W$  is the yield in kilotons. For detonation depths greater than  $21W^{1/3}$  feet, direct application of usual hydroacoustic methods may be employed. For underwater source depths shallower than  $21W^{1/3}$  feet, all of the water above the detonation is vaporized and new phenomena must be considered. The theory developed in Reference 1 relevant to the determination of a yield/altitude curve for atmospheric shots is predicated on the assumption that the detonation occurs at such height that the shock wave separates from the fireball (hydrodynamic separation) before interacting with the sea surface. In the atmosphere, hydrodynamic separation occurs at a range of  $15W^{1/3}$  feet, where  $W$  is the yield in kilotons. The atmospheric region, then, is that portion of the axis above  $15W^{1/3}$  feet. Thus, the near-surface region extends from  $21W^{1/3}$  feet in water to  $15W^{1/3}$  feet in air.

### 2.1.1 Yield Vs Depth - Underwater Case

The first step in the specification of the yield-vs-depth curve for an underwater shot is the determination of a source level-vs-depth curve based on the received acoustic signal. The determination of source level vs depth requires that, for the analysis frequency, the detonation site-to-receiver propagation loss be estimated for detonation depths throughout the water column. The source spectrum level at each depth is given by

$$SL = RL + PL \quad (1)$$

where

SL is the source spectrum level

RL is the received signal spectrum level

PL is the predicted propagation loss

Thus, the source level determination at any given assumed source depth is that level which would produce the actual received signal level if the detonation had occurred at the given depth. Because the classification system is intended for use in situations where the detonation site-receiver separations are quite large, and, therefore, where uncertainties in the detail of the propagation loss-vs-range function are large, broad range averaging - say 30 nm - will be employed in the propagation prediction process. The specification of an appropriate transmission loss model (or models) for incorporation into the classification system is beyond the scope of this study. Suffice it to state here that the prediction requirements can certainly be met through the use of one or more of the computer-implemented models currently available to the Navy.

The next computer step is the conversion of the source level-vs-depth curve, as determined above, to the corresponding yield-vs-depth curve. If the actual burst occurs in the atmosphere or at such depth in the ocean as

to result in the venting of the bubble formed by the detonation, the received underwater signal is the result of acoustic energy generated solely by the shock wave. If the burst occurs underwater below venting depth, the received signal reflects the sum of the energy generated by the shock wave and bubble pulse. However, the bubble pulse period for nuclear charges is so long that the energy contributed by the bubble is limited to very low frequencies. If we restrict the analysis to frequencies greater than about 10 Hz, the bubble energy is negligible and the received signal can be assumed to have been generated solely by the shock energy. Yield determinations can therefore be made using acoustic source level-vs-yield data based on the nuclear shock wave only. In this document, an analysis frequency of 20 Hz is assumed.

For detonations underwater, it can be shown that nuclear shock wave source levels vary approximately as  $7.5 \log W$ . Expressed another way, source levels change by 7.5 dB per order of magnitude change in yield. This relationship permits one to determine - for a given frequency - the yield of a detonation based on its source level and a known yield and source level used as a reference. The algorithm is given by

$$W = W_{REF} 10^{\left( \frac{SL - SL_{REF}}{7.5} \right)} \quad (2)$$

where

$W$  is the yield to be determined

$W_{REF}$  is the reference yield

$SL$  is the source level

$SL_{REF}$  is the reference yield source level

Based on information provided in Reference 2, it is found that for a 1-kiloton detonation the source level at 20 Hz is 268.4 dB/ $\mu$ Pa/Hz at 1 yard. Using 1 kiloton as the reference yield, Eq. (2) becomes

$$W = 10^{\left(\frac{SL - 268.4}{7.5}\right)} \quad (3)$$

where

W is the yield in kilotons

SL is the source level in dB//μPa/Hz at 1 yard

Eq. (3) is the algorithm to be used in determining the yield-vs-depth curve for the underwater case. The curve is terminated at that depth above which, for any given source depth, the value of  $21W^{1/3}$  is greater than the given depth.

#### 2.1.2 Yield Vs Altitude - Atmospheric Case

For an over-water nuclear detonation, there are two wave types which can penetrate the air-water interface and propagate to long range via RSR paths. These are the geometric wave and the lateral wave. The geometric wave is that wave whose propagation can be described by normal ray acoustic methods. The waterborne lateral wave results from the fact that exponentially decaying inhomogeneous plane waves present in the expansion of the spherical wave issuing from the detonation point, on interaction with the air-water interface directly below the detonation, excite the usual plane waves in the water, which are then propagated at all angles of incidence ( $\theta$ ) satisfying the condition  $\cos\theta > 1/n$ , where  $n$  is the index of refraction at the interface. It is only generated when the altitude of the detonation is such that at the ocean surface directly below the detonation the shock wave velocity is greater than the speed of sound in the water ( $n > 1$ ). In the design of the classification system it is assumed that the contribution of the lateral wave energy to the total signal received at long

range is negligible. That is, only the energy arriving via ray acoustic paths is treated. The ray acoustic paths of interest are those associated with the long range propagation modes. These are illustrated in Figure 1. The angle of incidence ( $\theta_i$ ) at the air-water interface is related to the angle of transmission ( $\theta_t$ ) at the interface by

$$\theta_i = \arccos (n \cos \theta_t) \quad (4)$$

where  $n$  is the index of refraction. The value of  $n$  at the interface is given by

$$n = \frac{\text{incident shock wave velocity}}{\text{speed of sound in water at the surface}} \quad (5)$$

Since the shock wave velocity varies (decreases) with range from the detonation point, the value of  $n$  at the interface varies (decreases) with slant range to the interface.  $\theta_{t(\min)}$  is a function of the near-surface sound speed maximum and is normally very small. When the maximum occurs at the surface (no surface duct),  $\theta_{t(\min)}$  is  $0^\circ$ .  $\theta_{t(\max)}$  is a function of sound speed at the ocean bottom and, for deep-water conditions, is typically on the order of 6 or 7 degrees.

The first computational step in the determination of the yield-vs-altitude curve is the development of a family of relative received level curves. Each of these curves shows, for a constant yield, received signal level as a function of altitude relative to that which would be received if the source were located at some reference position on the depth/altitude axis. The reference position as defined here is that depth within the water column at which the propagation loss to the receiver location is minimized. For a source in deep water, this depth will be that of the deep sound channel axis. An equation for determining relative received level for the deep-water case was developed in Reference 1 and is presented below.

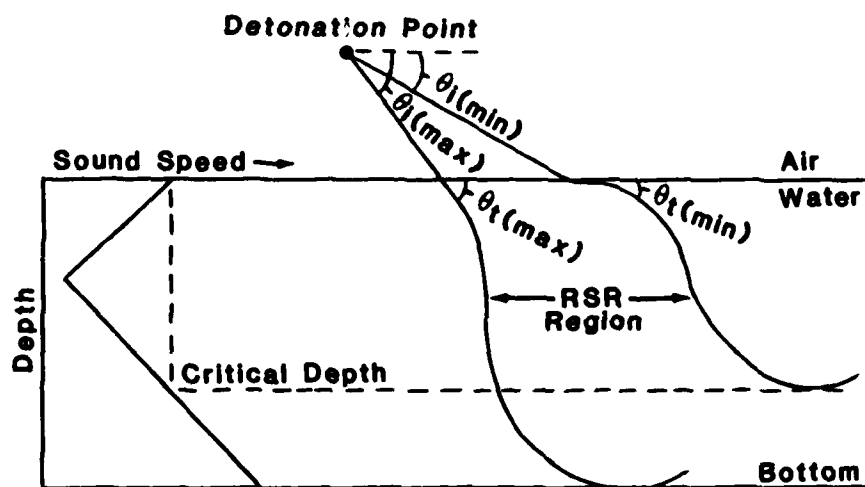


Figure 1. Ray Acoustics Paths of Interest.

$$\text{RRL} = 10 \log \left[ 9.255 \times 10^{-13} [n^2 / (1-n^2)] [P_s^2 \delta^2 W^{-0.753}] [\theta_s^3 / \theta_{sc}] \right] \quad (6)$$

where,

RRL is the relative received level in dB.

$\delta$  is the slant range, in feet, from the air detonation to the region on the ocean surface where the ray acoustics energy enters the water.

$n$  is the index of refraction at the air-water interface at slant range  $\delta$ .

$P_s$  is the peak overpressure, in psi, at slant range  $\delta$ .

$W$  is the detonation yield in kilotons.

$\theta_s$  is the maximum transmission angle at the surface for RSR propagation, in radians.

$\theta_{sc}$  is the maximum angle of inclination at the sound channel axis associated with the long range propagation modes (RRR and RSR), in radians.

Eq.(6) is based on the assumption that the index of refraction does not vary with range across the region within which the energy propagated via RSR paths enters the water. At high altitudes, where  $n \ll 1$ , the assumption of a constant  $n$  is valid. However, for near-surface detonations, as  $n$  approaches 1, the equation breaks down and corrections to account for variations in  $n$  must be made.

In Reference 1, numerical values of RRL based on Eq. (6) were provided, assuming a standard deep-ocean environment.\* The assumed sound speed as a function of depth is shown in Figure 2. The sound speed is 5037 ft/sec at the surface, 4900 ft/sec at the sound channel axis (4000 ft) and 5074 ft/sec at

---

\*It should be noted that the derivation of Eq. (6) involved the assumption of a standard atmosphere, the properties of which are described in Reference 1.



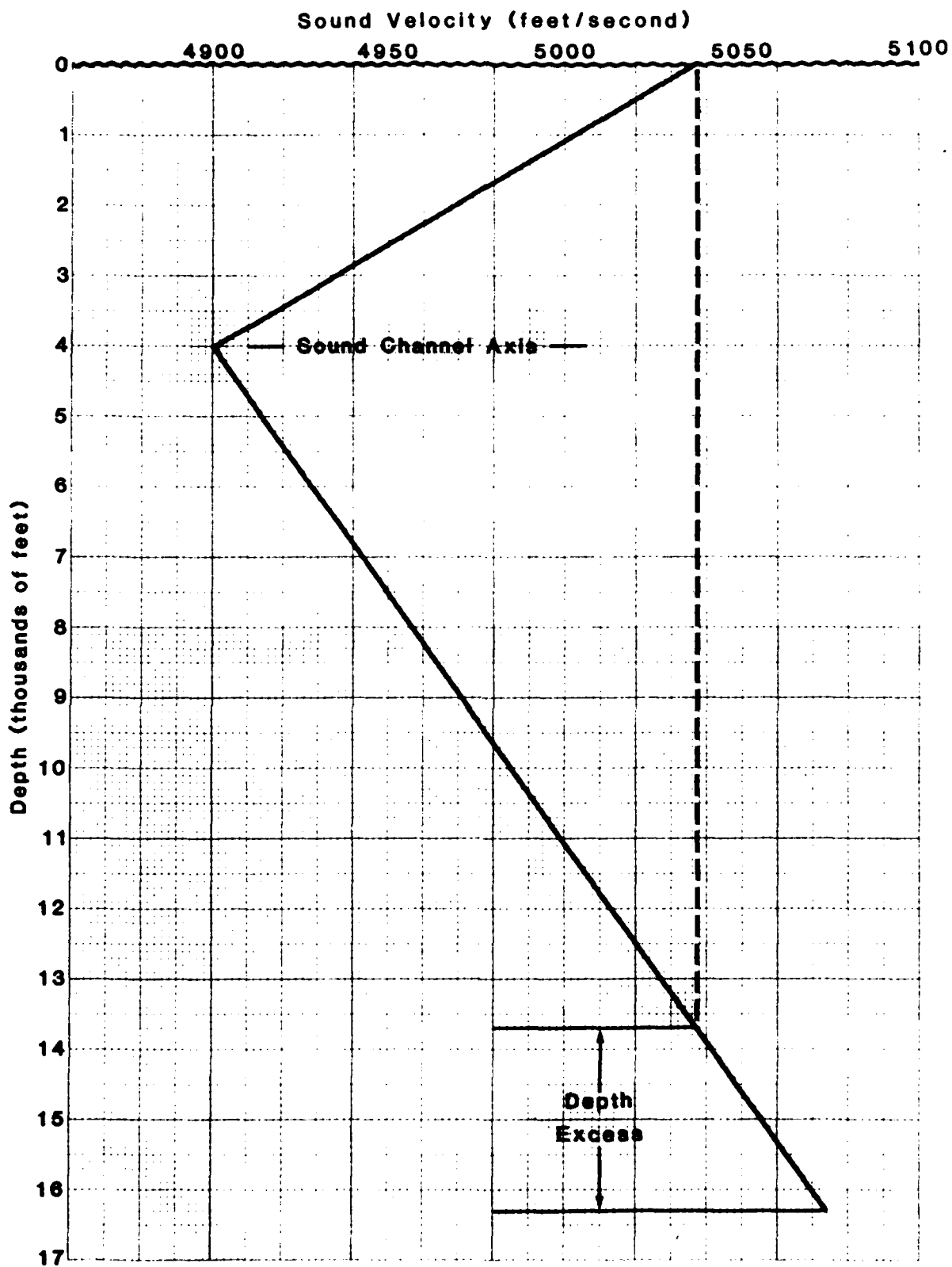


Figure 2. The Sound Velocity Profile for the Standard Ocean.

the bottom (16,400 ft). The depth excess is approximately 2640 ft. The values of  $\theta_s$  and  $\theta_{sc}$  for this profile are  $6.92^\circ$  and  $15.05^\circ$ , respectively. Figure 3 shows the results for a 1-kiloton detonation. The curve has been corrected at the lower altitudes to account for variations in  $n$  with range. Results for any other yield may be obtained by a simple  $W^{1/3}$  scaling procedure. For a yield  $W$ , the altitude of each point on the curve is multiplied by  $W^{1/3}$ . Then, each point on the new curve is shifted in level by adding  $-0.87 \log W$  dB to the relative received level.

The family of RRL curves will consist of thirty-six curves extending from  $10^{-2}$  to  $10^5$  kilotons. The yield associated with each curve will differ by a factor of  $10^{1/5}$  from the yields for adjacent curves. Thus, in ascending order beginning with 0.01 kilotons, the yields, in kilotons, associated with the first eleven curves are: 0.01, 0.0158, 0.0251, 0.0398, 0.0631, 0.1, 0.158, 0.251, 0.398, 0.631 and 1. Using the standard ocean environment, the RRL curves for every fifth yield in the family have been determined (scaled from the 1-kiloton curve) and are presented in Figure 4. Each curve is terminated at an altitude of 5000 feet, which corresponds to the approximate maximum altitude of applicability of the standard atmosphere assumed in the theoretical developments upon which this study is based.

From Eq. (6) it is seen that the RRL curve varies as the cube of  $\theta_s$  - a strong functional dependence. Since  $\theta_s$  is a sensitive function of surface sound speed and bottom depth and can exhibit marked spatial and temporal variability, it is evident that large variations from the results given in Figure 4 can occur, due to variations in this one parameter, depending on the time and location of a detonation. As a conservative example, in one deep-water region off the U.S. east coast, it is estimated that over the

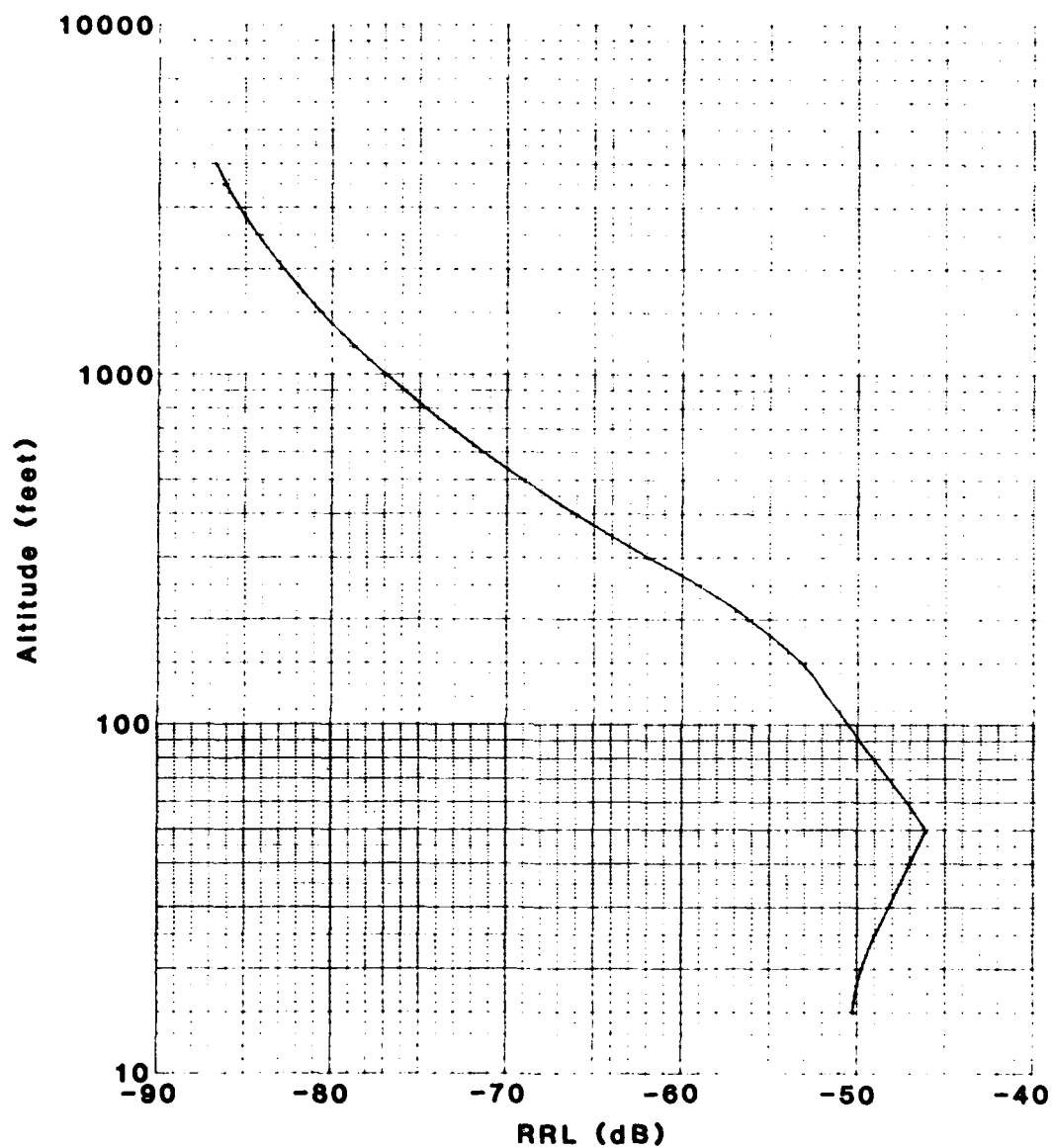


Figure 3. Relative Received Level (RRL) Versus Altitude for a 1-Kiloton Detonation - Atmospheric Region - Standard Ocean.

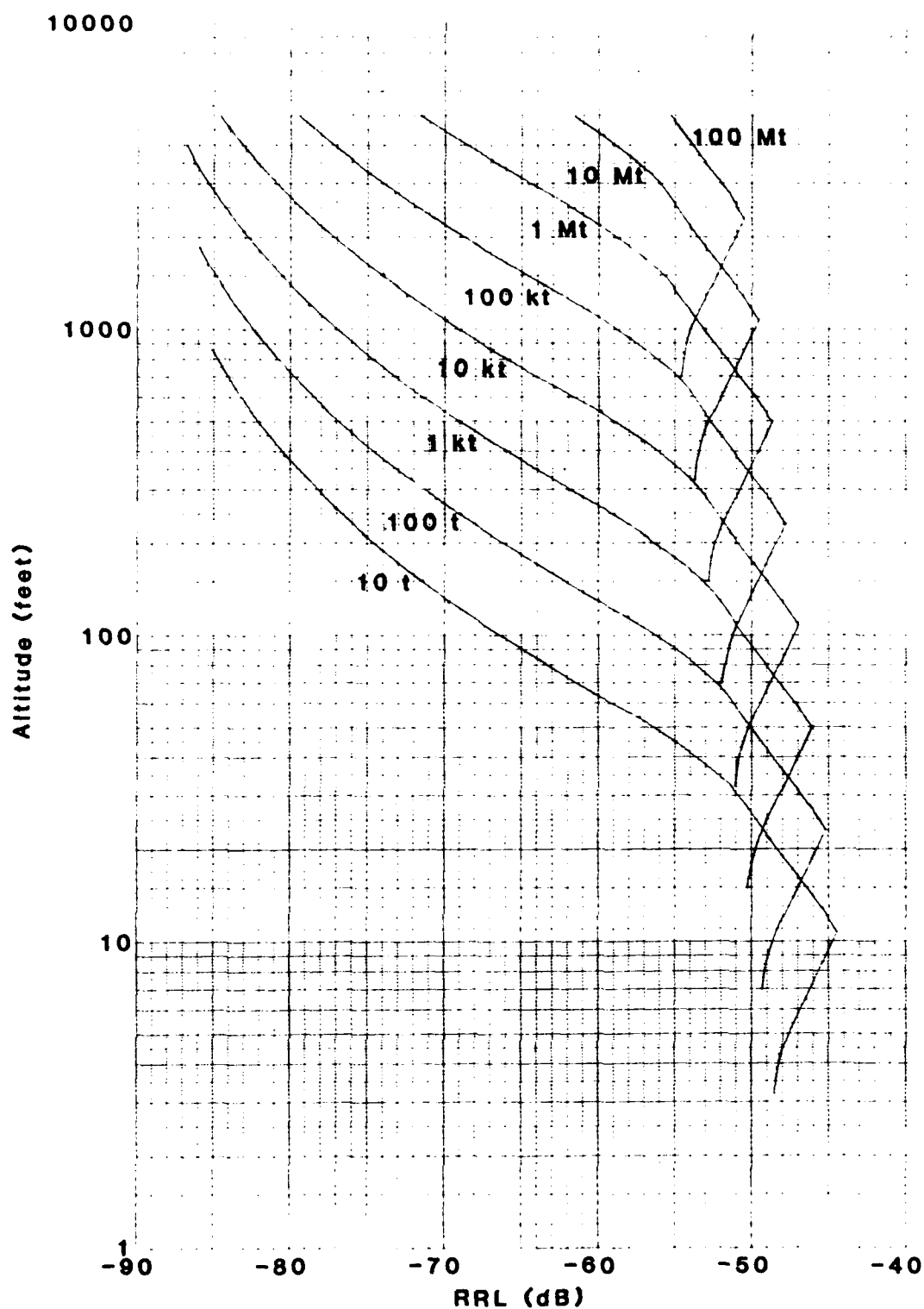


Figure 4. Relative Received Level (RRL) Versus Altitude for Every Fifth Yield in Yield Family - Atmospheric Region - Standard Ocean.

course of a year  $\theta_s$  varies from  $4.26^\circ$  to  $11.3^\circ$ . This corresponds to variations in RRL of 13 dB.

On a worldwide basis, surface sound speeds vary by no more than about 7% throughout the year. Hence, the value of  $n$  for a given peak overpressure will never vary by more than about 7%. The values of  $\delta$  and, hence,  $P_s$ , which depend on surface sound speed, also are not expected to change appreciably, on a percentage basis, from one environment to another. Thus, the expectation is that for any environment other than that for the standard ocean, the difference in RRL for any given altitude will be determined almost entirely by the change in  $\theta_s$  from that for the standard ocean, with a relatively small, but, perhaps significant contribution due to the change in  $\theta_{sc}$ . And, indeed, sample calculations performed by the authors demonstrate this to be the case. This permits a simple scaling procedure to be employed whereby the results obtained for the standard ocean can be converted to RRL for any other environment simply by adding a correction value, involving  $\theta_s$  and  $\theta_{sc}$  only, to the standard ocean levels. This correction is given by

$$\Delta RRL = 21.73 + 10 \log (\theta_s^3 / \theta_{sc}) \quad (7)$$

where

$\Delta RRL$  is the correction factor in dB

$\theta_s$  and  $\theta_{sc}$  are the surface and sound channel angles for the new environment, in radians

Since  $\Delta RRL$  is independent of altitude the effect of the scaling is simply the shift of the entire standard ocean relative received level curve by  $\Delta RRL$ .

The methodology to be employed for the determination of  $\theta_s$  and  $\theta_{sc}$  for a given event, described below, is based on the assumption that the geometric spreading of the shot-generated acoustic energy in the vicinity of the receiving sensor is essentially cylindrical; that is, that the receiver is

at long range from the detonation. This assumption is not believed to be valid from the general usefulness of the system in view of the strong expectation that, for a given event, the detonation/receiver separation range will be large - perhaps thousands of miles.

Long range propagation loss within the deep sound channel may be approximated by assuming spherical spreading out to some transition range  $R_0$  followed by cylindrical spreading thereafter. The loss, as a function of range, is given by

$$PL = 10 \log R_0 + 10 \log R + \alpha R$$

where

PL is the propagation loss in dB

$R_0$  is the transition range in yards

R is the source/receiver separation range in yards

$\alpha$  is the absorption coefficient in dB/yd

The transition to cylindrical spreading results from the interaction of acoustic energy propagating outward from the source with the ocean surface and bottom boundaries which serve to trap the energy within the water column. In reality, of course, the transition from spherical to cylindrical spreading is gradual and does not occur abruptly at a discrete range.  $R_0$  is simply a range within the transition region which yields reasonable predictions of propagation loss. Consider the illustration shown as Figure 5. In Figure 5 the receiver is located at mid-column for illustrative purposes only. The angle  $\theta$  represents the maximum inclination angle associated with the long range propagation modes as would be determined from the sound speed profile. Dashed curves represent the refracted paths associated with  $\theta$ , while straight line paths ignore refraction. For this study,  $R_0$  is taken as a range at which the vertical separation of the straight line paths is

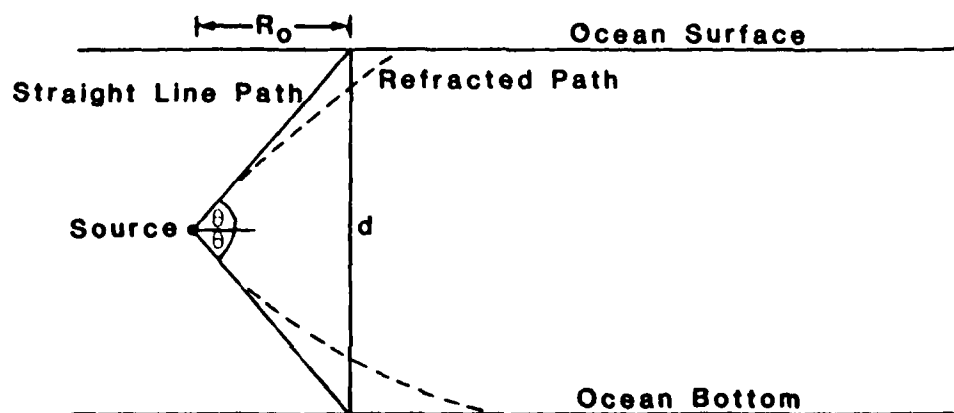


Figure 5. Diagram Illustrating the Relationship Between the Spherical Spreading-to-Cylindrical Spreading Transition Range ( $R_0$ ), the Water Depth ( $d$ ) and the Maximum Inclination Angle at the Source ( $\theta$ ) Associated With the Long-Range Propagation Modes. (See text.)

with  $\theta$  equals the water depth ( $d$ ). This reasonably estimates the range at which the channeling effect of the ocean boundaries begins to take effect.

$R_0$  is then given by

$$R_0 = d/2 \tan \theta \quad (9)$$

Substituting the expression for  $R_0$  in Eq. (8), we obtain

$$PL = 10 \log (d/2 \tan \theta) + 10 \log R + \alpha R \quad (10)$$

For a known propagation loss obtained at long range, an estimate of the angle  $\theta$  at the source may be obtained by solving Eq. (10) for  $\theta$ . The resulting equation is given by

$$\theta = \arctan \left( \frac{d}{2} \times 10^{\frac{PL - 10 \log R - \alpha R}{10}} \right) \quad (11)$$

If the known propagation loss is obtained for a surface source, a 3-dB correction must be applied to Eq. (10) to account for the absence of upgoing energy at the source. The loss is then given by

$$PL = 10 \log (d/2 \tan \theta) + 10 \log R + \alpha R + 3 \quad (12)$$

and  $\theta$  is given by

$$\theta = \arctan \left( \frac{d}{2} \times 10^{\frac{PL - 10 \log R - \alpha R - 3}{10}} \right) \quad (13)$$

The values of  $\theta_{sc}$  and  $\theta_s$  for use in the determination of the RRL curves for the atmospheric case will be determined using Eqs. (11) and (13), respectively. The PL inputs to the equations are obtained from the set of propagation loss computations which were obtained for assumed source positions throughout the water column (Section 2.1.1). The PL input for the determination of  $\theta_{sc}$  (Eq. (11)) is the loss obtained for an on-axis source - if a deep channel axis is present. If a deep axis is not present, the PL input to Eq. (11) is the minimum predicted loss within the water column. The value of PL to be used in the determination of  $\theta_s$  is that obtained for a



surface source. The water depth ( $d$ ) is assumed to be that at the receiver site. The values obtained for  $\theta_{sc}$  and  $\theta_s$  are equivalent to the angles which would be obtained for the predicted PL values if the water depth along the entire propagation track (detonation site to receiver) was equal to that at the receiver site and if the acoustic bottom loss along the track was infinite. The characteristics of the actual environment (sound speed structure, bottom loss, bathymetry, etc.) are reflected in the computed values of  $\theta_s$  and  $\theta_{sc}$  through the PL input.

The determination of the RRL curves, then, comprises three steps. Step 1 is to scale the 1-kiloton standard ocean RRL curve to the thirty-five other yields in the RRL curve family (scaling: altitude multiplied by  $W^{1/3}$  followed by a shift of  $-0.87 \log W$  dB). Step 2 is to determine  $\theta_s$  and  $\theta_{sc}$  for the subject environment using Eqs. (11) and (13). Step 3 is to scale the standard ocean RRL curves obtained in Step 1 to the subject environment, using Eq. (7).

The next computational step, once the RRL curves in the subject environment have been determined, is to normalize the RRL curves such that, for any given normalized curve (NRRL), the NRRL values represent levels relative to the level which would be received for a 1-kiloton detonation on axis (or, the depth at which the detonation site-to-receiver propagation loss is minimized). For each RRL curve, the normalization is performed by adding  $7.5 \log W$  dB to the RRL values, where  $W$  is the yield, in kilotons, for which a given curve was computed. This results in a shift of  $7.5 \log W$  dB to the entire RRL curve. For example, for the 100-kiloton RRL curve, the normalization factor is  $7.5 \log 100$ , or, +15 dB. At any given altitude, then,  $NRRL = RRL + 15$  dB. The correction for each curve merely reflects the difference in source level between that of an underwater shot of yield  $W$  and

that of an underwater 1-kiloton detonation. Corrections range from -15 dB for the 0.01-kiloton curve to +37.5 dB for the  $10^5$ -kiloton curve.

The determination of the yield-vs-altitude curve for the subject environment is based directly on the NRRL curve family. Let us assume, for discussion purposes, that, for a particular case the subject environment is identical to that of the standard ocean environment. The NRRL curves for this case are as shown in Figure 6. For presentation purposes, only every fifth curve in the total family of curves is presented in the figure. Let us also assume that on the underwater yield-vs-depth curve for a particular event occurring in this environment, the yield at the reference depth has been determined to be 0.02 lb ( $10^{-8}$  kiloton). The received level for this yield is, then, -60 dB ( $7.5 \log 10^{-8}$ ) relative to the level that would be received if the yield at the reference depth were 1 kiloton. Then, for any given NRRL curve the yield/altitude pairing at the point on the curve for which NRRL equals -60 dB defines a point on the yield-vs-altitude curve, and the set of points defines the yield-vs-altitude curve. In Figure 6, the yield-vs-altitude curve for this example is determined by the points indicated by the heavy dots along the vertical line at -60 dB. The yield-vs-altitude plot for this data is shown in Figure 7. The curve definition is, of course, not nearly as good as it would be if the full set of NRRL curves was used.

It is important to note that the 1-kiloton normalization may be performed before, rather than after, the environmental correction to the standard ocean (Eq. (7)) has been applied. That is, the normalization may be performed on the standard ocean RRL curve family, and the environmental correction applied to the resulting standard ocean NRRL curves to obtain NRRL in the subject

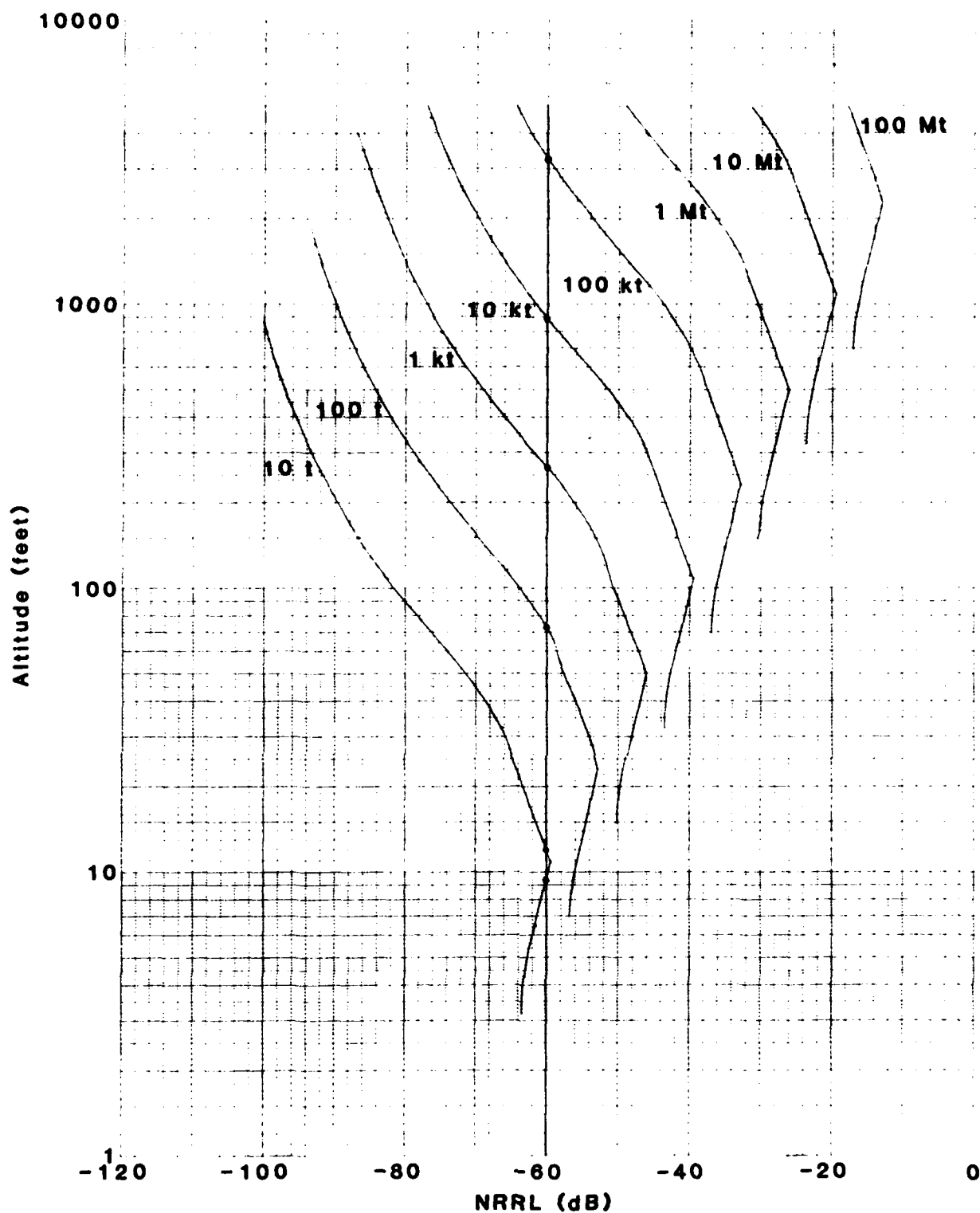


Figure 6. Normalized Relative Received Level (NRRL) Versus Altitude for Every Fifth Yield in Yield Family - Atmospheric Region - Standard Ocean.

(Heavy dots along vertical line at -60 dB indicate yield/altitude combinations for a 0.02 lb charge on axis. See text.)

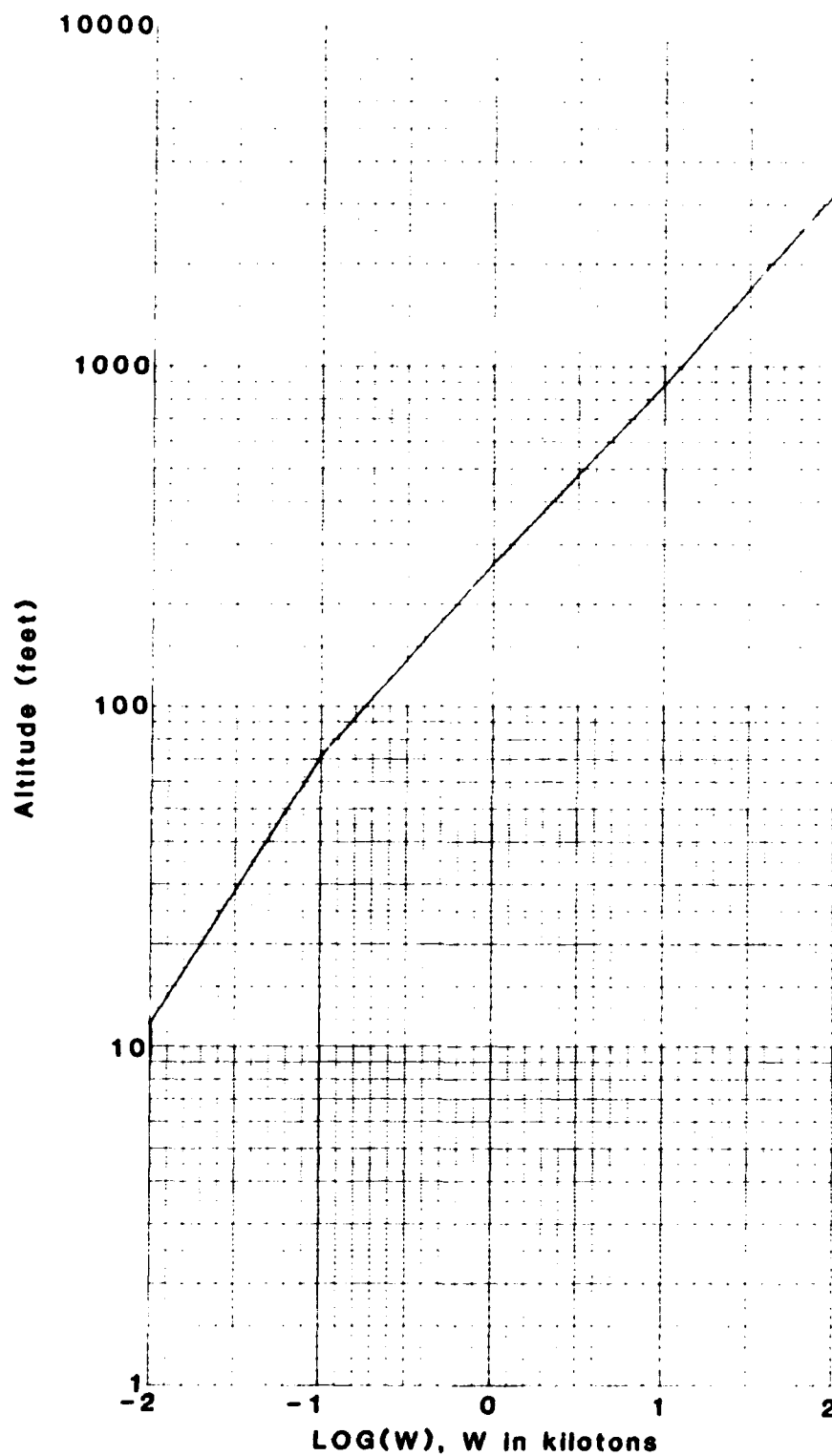


Figure 7. Yield Versus Altitude for a 0.02 lb Charge on Axis  
- Atmospheric Region - Standard Ocean.

environment. When the classification system is implemented, the NRRL curves for the standard ocean will be permanently stored within the computer. Then, for a given application of the system the only computational tasks required for the determination of the yield-vs-altitude curve in the atmosphere are:

- (1) determine  $\theta_s$  and  $\theta_{sc}$  for the subject environment; (2) apply the environmental correction, Eq. (7), to the standard ocean NRRL curves to obtain NRRL curves for the subject environment; (3) determine the received level for the reference-depth yield on the underwater yield-vs-depth curve relative to that which would be received by a 1-kiloton detonation at the reference depth; (4) specify the yield-vs-depth curve by the determination of yield/altitude points within the NRRL curve family for which the value of NRRL is that determined in the previous step.

### 2.1.3 Yield Vs Depth/Altitude - Near-Surface Case

#### 2.1.3.1 Above-Surface Region

In this section we specify the methodology for the determination of yield vs altitude over the region of the altitude axis for which the height associated with any given yield on the yield-vs-altitude curve is less than the range for hydrodynamic separation. Within the near-surface region the water participates in the formation of the fireball and a shock wave is generated in the water medium as in the case of an underwater detonation. This is a very efficient mode of excitation since it does not involve the losses associated with the impedance mismatch between air and water. A complete discussion of the theory underlying the methodology to be employed here will not be presented. Rather, the reader is referred to Reference 3 which presents a complete treatment.

The first step in the computational process is the development of a family of RRL curves. As for the atmospheric case, the RRL curve family will consist of thirty-six curves extending from  $10^{-2}$  to  $10^5$  kilotons, with each curve differing by a factor of  $10^{1/5}$  in yield from the yields for adjacent curves.

For a shot occurring in the air at an altitude less than the range for hydrodynamic separation, there is penetration of the fireball into the water. The depth of penetration is inversely related to shot altitude. The fraction of the total energy available for formation of the shock wave in the water is just that fraction of the fireball energy which penetrates the air-water interface. This directly induced shock wave energy, normalized to the induced energy of a detonation occurring at the air-water interface, is shown as a function of scaled detonation altitude in column 2 of Table 1. The scaled altitude values are equal to altitude (H) divided by hydrodynamic separation range ( $R_a$ ). The values range from 0 dB at the normalization point to  $-\infty$  dB at the altitude corresponding to  $R_a$ , and are assumed to be environmentally independent. The RRL for a surface detonation is assumed here to be -11.1 dB, independent of yield and environmental conditions. The determination of this value is based on three considerations. First, using the standard ocean environment, it was determined that, based on the solid angles at the source associated with long range propagation, the received level for an explosive source just below the ocean surface is -3.4 dB relative to the level that would be received from an on-axis source of equal yield. For a source right at the surface the received level will be reduced an additional 3 dB due to the absence of initially upgoing energy at the source, yielding a relative level of -6.4 dB. Based on data obtained for small HE charges at the air-water interface it is estimated that directly below a surface charge the

Table 1. Directly Induced Shock Wave Energy as a  
Function of Scaled Detonation Altitude

(1) Scaled Detonation Altitude ( $H/R_a$ )	(2) Directly Induced Shock Wave Energy Relative to That of a Surface Detonation (dB)	(3) RRL (dB)
0	0.0	-11.1
0.1	- 0.7	-11.8
0.2	- 1.5	-12.6
0.3	- 2.5	-13.6
0.4	- 3.7	-14.8
0.5	- 4.9	-16.0
0.6	- 6.4	-17.5
0.7	- 9.2	-20.3
0.8	-12.5	-23.6
0.9	-18.4	-29.5
1.0	- $\infty$	- $\infty$

shock wave energy flux will be 34% of the energy for an underwater detonation. Thus, an additional correction of -4.7 dB is required, yielding the total RRL of -11.1 dB for a surface detonation. It is seen from the above discussion that RRL for a surface source is not truly environmentally independent. However, it is not expected that this assumption will lead to significant errors in foreseeable real-world situations.

RRL as a function of scaled altitude is shown in column 3 of Table 1. These values were obtained simply by adding -11.1 dB to the relative directly induced energy levels given in column 2. RRL as a function of absolute altitude for a 1-kiloton detonation is shown in Figure 8. These results may be scaled to any other yield by simple  $W^{1/3}$  scaling. That is, for any yield  $W$ , expressed in kilotons, the altitude of each point on the 1-kiloton curve is multiplied by  $W^{1/3}$ . The RRL curves for every fifth yield in the curve family are presented in Figure 9. It should be noted that each curve is terminated at that altitude for which the value of RRL is equal to RRL at the lowest altitude (hydrodynamic separation range) on the corresponding atmospheric RRL curve (see Figure 4). The implemented classification system will simply ignore the small gap introduced by this truncation as its inclusion can produce spurious, physically unmeaningful results in the determination of yield vs altitude.

Once the RRL curve family has been developed, the process of determining yield vs altitude in the near-surface region proceeds in precisely the same fashion as for the atmospheric case except that there is no environmental correction to consider. Specifically, the remaining computational steps are: (1) develop a family of NRRL curves; (2) determine the value of NRRL for the reference depth yield, and (3) specify the yield-vs-altitude curve in the near-surface region by the determination of yield/altitude points within the



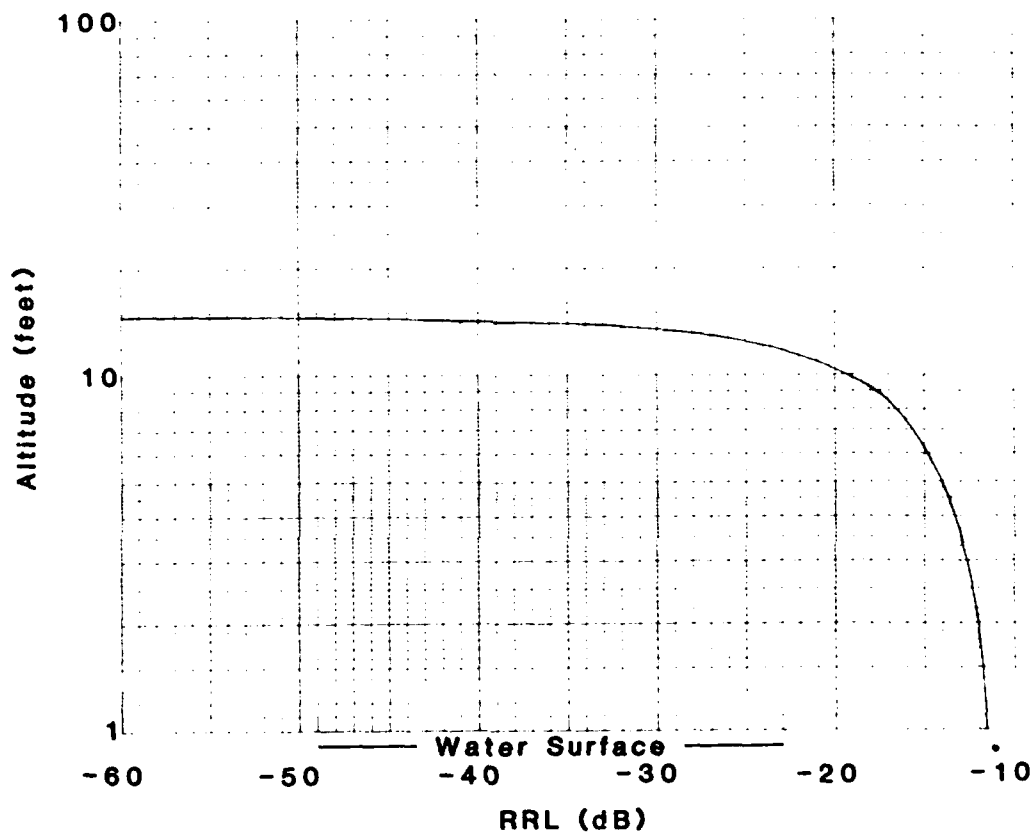


Figure 8. Relative Received Level (RRL) Versus Altitude for a 1-Kiloton Detonation - Near-Surface Region.

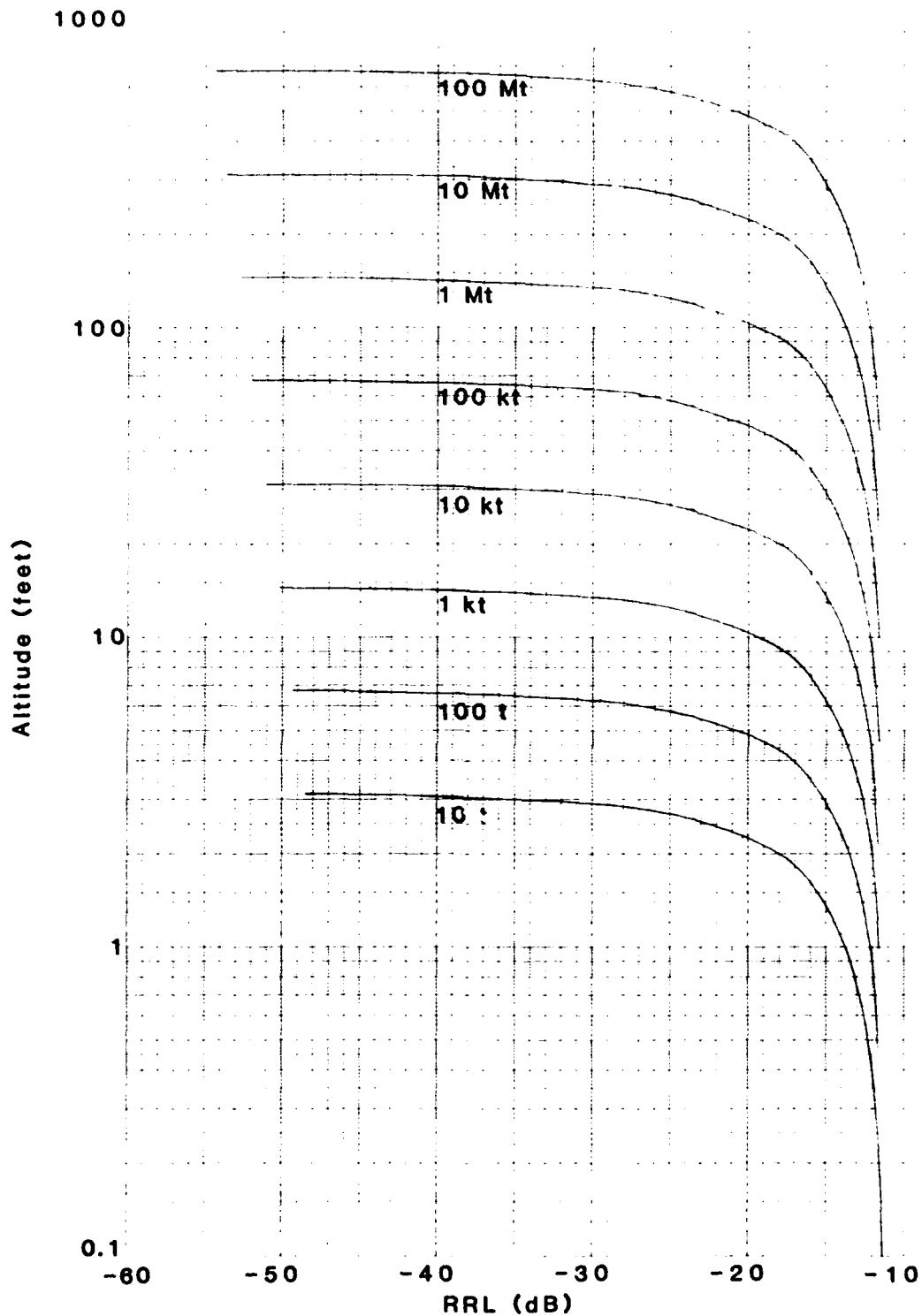


Figure 9. Relative Received Level (RRL) Versus Altitude for Every Fifth Yield in Yield Family - Near-Surface Region.

NRRL curve family for which the value of NRRL is that determined for the reference depth yield. NRRL has precisely the same definition here as given in Section 2.1.2 and is determined in precisely the same fashion. NRRL curves for the near-surface region are presented in Figure 10. Again, for presentation purposes, only every fifth curve in the family of curves is presented.

Sample yield-vs-altitude curves combining the near-surface and atmospheric regions are presented in Figure 11. For the atmospheric region, determinations were based on the standard environment. Curves are shown for seven reference depth yields ranging from 0.02 lb to 1 kiloton. The curves are based on the set of NRRL curves consisting of every fifth curve of the near-surface and atmospheric curve families. When the classification system is implemented, the near-surface NRRL curves will be permanently stored within the computer. Then, for a given application of the system the only computational tasks required for the determination of yield-vs-altitude in the near-surface region will be steps 2 and 3 above.

The development of the methodology for determination of yield vs depth/altitude has led to an important general conclusion relative to the classification of a detonation. If we consider the practical minimum yield of a test nuclear charge to be about 10 tons (NRRL = -15 dB), then, for a given detonation-like signal which indicates a possible underwater nuclear detonation (>10 tons on the yield-vs-depth curve), one can conclude with a high degree of confidence that the signal was not generated by an atmospheric blast (altitude  $>15W^{1/3}$  ft). The rationale for this conclusion is that the generation of such a large underwater signal would require an impractically high atmospheric yield. However, the possibility that the detonation occurred in the near-surface region could not be ruled out.

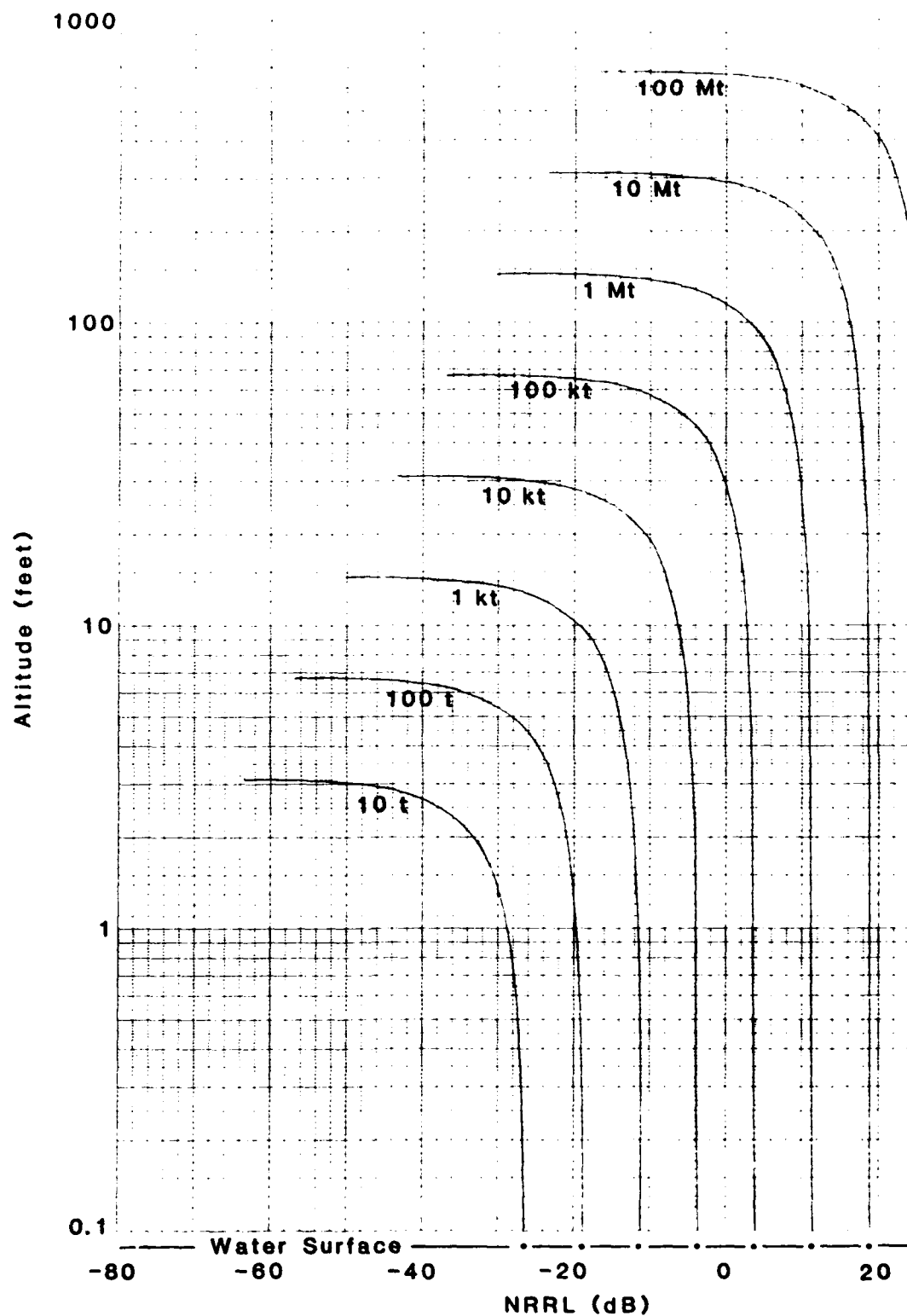


Figure 10. Normalized Relative Received Level (NRRL) Versus Altitude for Every Fifth Yield in Yield Family Near-Surface Region.

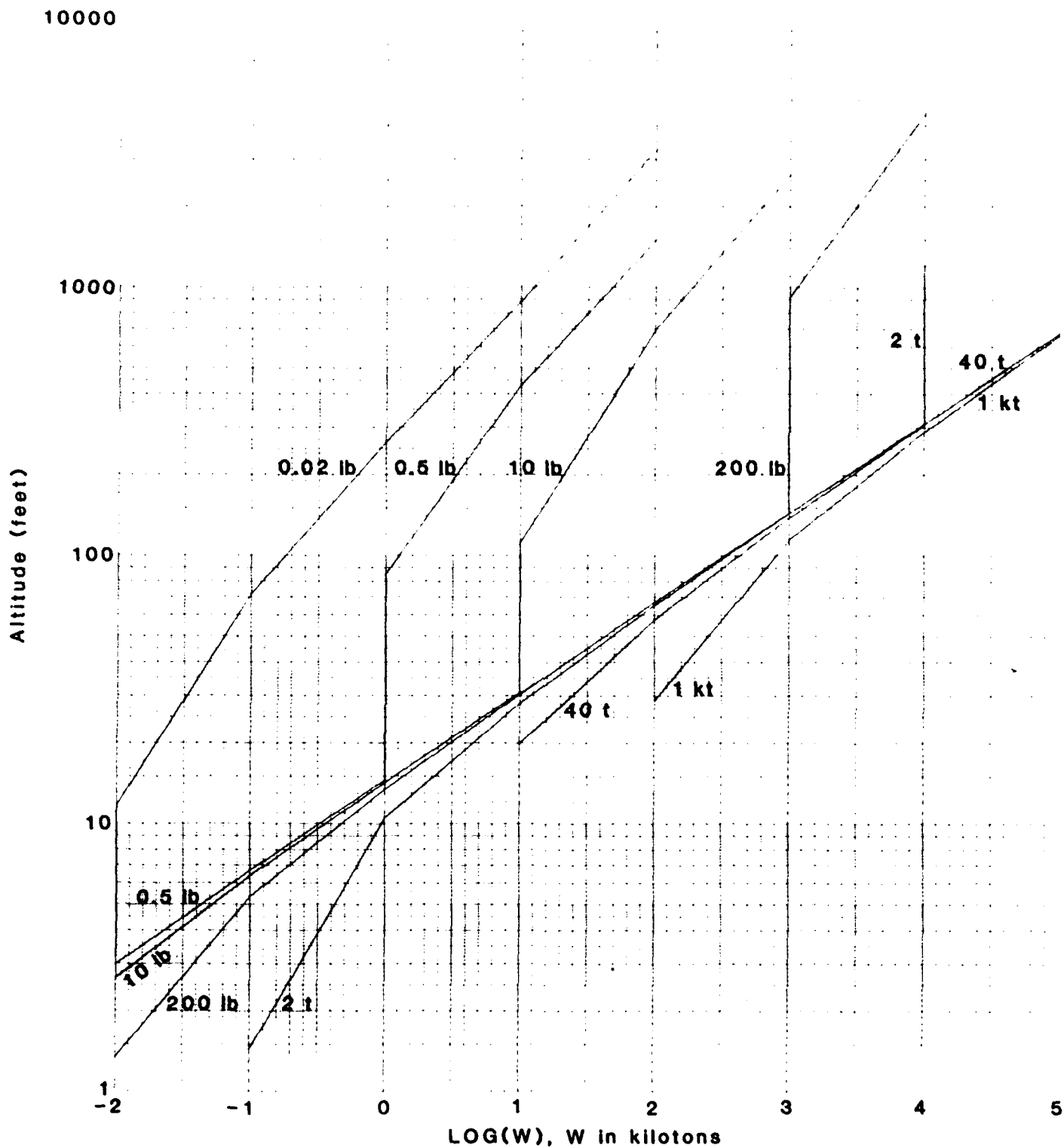


Figure 11. Yield Versus Altitude for Indicated On-Axis Yields - Near-Surface and Atmospheric Regions - Standard Ocean.

#### 2.1.3.2 Below-Surface Region

As previously discussed, the underwater near-surface region is defined as that portion of the water column shallower than  $21W^{1/3}$  feet, where  $W$  is the detonation yield in kilotons. Within this region all of the water above the detonation is vaporized. To date, no phenomenologically based methodology for the determination of RRL at near-surface depths has been devised. The classification system will determine yield vs depth within the near-surface region by simple linear interpolation. That is, yield/depth pairings will be linearly interpolated based on the yield/depth combination at the terminus of the underwater yield-vs-depth curve and the yield obtained for a surface source. The surface yield is given by

$$W_{SUR} = 30.2 W_{RD} \quad (14)$$

where

$W_{SUR}$  is the surface yield

$W_{RD}$  is the reference depth yield

#### 2.2 Signal Processing

The signal from a nuclear underwater/air burst is assumed to be received on a single hydrophone located within the deep sound channel. It is further assumed that the underwater sound path between the burst and the receiving hydrophone is long (~2000 nm) and will support RRR and/or RSR propagation. The time constant of the positive overpressure pulse at the receiving hydrophone is short (~one second, maximum), but, because of the arrival time dispersion of the signal propagating along the many multipaths, the received signal consists of a series of overlapping pulses that at long ranges may persist for many seconds. This time dispersion varies with range; at a range of 2000 nm in the deep ocean, it is approximately 15 seconds. The operational

frequency passband of the receiver is 10 to 30 Hz, a bandwidth of about 1.6 octaves. The signal within this passband will have a spectrum slope of -6 dB/octave for underwater bursts and for high yield air bursts, a spectrum slope of 0 dB/octave for moderate yield, moderate altitude air bursts and a spectrum slope of +6 dB/octave for low yield air bursts. Most of the yield/altitude combinations for which bursts can be detected fall into the -6 dB/octave spectrum slope category which will be the basis of the following signal processing analysis. The absorption loss in the 10 to 30 Hz passband is negligibly small and has no effect on the signal spectrum slope.

The initial signal detection can best be obtained by a broadband square law (auto-correlator) detector. The output signal-to-noise likelihood ratio is given by

$$\left(\frac{S}{N}\right)_{OUT} = \frac{\left( T \int_{f_1}^{f_2} F \cdot S_{IN} df \right)^2}{T \int_{f_1}^{f_2} (F \cdot N_{IN})^2 df} \quad (15)$$

where

$S_{IN}$  is the signal spectrum level at the detector input

$N_{IN}$  is the noise spectrum level at the detector input

$F$  is the passband shaping filter function

$f_1$  is the lower frequency of the passband

$f_2$  is the upper frequency of the passband

$T$  is the averaging time of the detected output signal

If the shaping filter is proportional to  $S_{IN}/N_{IN}^2$ , it is the optimum filter and Eq. (15) reduces to

$$\left(\frac{S}{N}\right)_{OUT} = T \int_{f_1}^{f_2} \left(\frac{S}{N}\right)_{IN}^2 df \quad (16)$$

The deep water noise level in the 10 to 30 Hz passband for an area of light-to-moderate shipping noise is approximately given by

$$N_{IN} = 86 - 10 \log f, \text{ dB re } 1\mu\text{Pa/Hz} \quad (17)$$

The signal level at the hydrophone receiver for an underwater nuclear detonation at the depth for minimum propagation loss is

$$S_{IN} = SL - PL_{MIN}, \text{ dB re } 1\mu\text{Pa/Hz} \quad (18)$$

where

SL is the spectrum source level of the detonation in dB re  $1\mu\text{Pa/Hz}$  at 1 yard

$PL_{MIN}$  is the propagation loss from source to hydrophone receiver in dB. The spectrum source level (SL) in the 10 to 30 Hz passband for a 1-kiloton underwater detonation is  $294 - 20 \log f$ , dB. Since the normalized relative received level (NRRL) gives the source level of any nuclear detonation relative to an underwater detonation of 1-kiloton yield, the spectrum source level can be expressed as

$$SL = 294 - 20 \log f + NRRL, \text{ dB re } 1\mu\text{Pa/Hz at 1 yard} \quad (19)$$

Thus, the signal level at the receiver input is

$$S_{IN} = 294 - 20 \log f + NRRL - PL_{MIN}, \text{ dB re } 1\mu\text{Pa/Hz}; \quad (20)$$

the signal-to-noise ratio at the receiver input is

$$\left(\frac{S}{N}\right)_{IN} = 208 - 10 \log f + NRRL - PL_{MIN}, \text{ dB}, \quad (21)$$

and the detected output signal-to-noise ratio for an averaging time  $T$  of 15 seconds and a passband of 10 to 30 Hz is, from Eqs. (16) and (21),



$$\begin{aligned}
 \left(\frac{S}{N}\right)_{\text{OUT}} &= 416 - 2 PL_{\text{MIN}} + 2 \text{NRRL} + 10 \log 15 \int_{10}^{30} \frac{df}{f^2}, \text{ dB} \\
 &= 416 - 2 PL_{\text{MIN}} + 2 \text{NRRL}, \text{ dB}
 \end{aligned}
 \tag{22}$$

The minimum level of NRRL that can be reliably detected is determined by a desired probability of detection, together with an allowed probability of false alarm per averaging time interval (T). A measure of these joint probabilities is a parameter called the detection index (d) which can be obtained from a set of Receiver Operating Characteristic (ROC) curves. The conventional ROC curves assume a steady signal over the averaging time, stationary Gaussian noise, a large time-bandwidth processing gain and no interfering signal-like noises. Whenever these conditions are not all met, a higher detection index is required. For this application (the detection of nuclear detonations) the signal is usually not steady over the averaging time because of the many multipaths with varying transmission losses; the noise in the 10 to 30 Hz passband is both non-stationary and too spiky to be Gaussian; the time-bandwidth gain is too small; and, shipping noises will often cause interference problems. Because of all these factors, a rather large detection index is recommended. Using Eq. (22), let  $\left(\frac{S}{N}\right)_{\text{OUT}} = d = 23 \text{ dB}$  and solve for the minimum detectable value of NRRL. Thus,

$$\text{NRRL}_{\text{MIN}} = \frac{1}{2} (23 - 416 + 2 PL_{\text{MIN}}) = PL_{\text{MIN}} - 196.5, \text{ dB}
 \tag{23}$$

The absolute value of signal output, using Eq. (20) for  $S_{\text{IN}}$ , is

$$S_{\text{OUT}} = 20 \log T \int_{f_1}^{f_2} S_{\text{IN}} df, \text{ dB re } 1 \mu\text{Pa}^2$$

$$\begin{aligned}
&= 588 - 2 PL_{\text{MIN}} + 2 \text{NRRL} + 20 \log 15 \int_{10}^{30} \frac{df}{f^2}, \text{ dB re } 1\mu\text{Pa}^2 \\
&= 588 - 2 PL_{\text{MIN}} + 2 \text{NRRL}, \text{ dB re } 1\mu\text{Pa}^2
\end{aligned} \tag{24}$$

At the minimum detectable level of NRRL,

$$(S_{\text{OUT}})_{\text{MIN}} = 588 - 2 \cdot 196.5 = 195 \text{ dB re } 1\mu\text{Pa}^2 \tag{25}$$

Whenever there is no signal the detected and averaged output is that due to only the ambient noise. Its level is

$$N_{\text{OUT}} = 20 \log T \int_{f_1}^{f_2} N_{1N} df = 172 + 20 \log 15 \int_{10}^{30} \frac{df}{f} = 189 \text{ dB re } 1\mu\text{Pa}^2 \tag{26}$$

Note that  $N_{\text{OUT}}$  is 6 dB less than  $(S_{\text{OUT}})_{\text{MIN}}$ . For a processor using the output of a single omnidirectional hydrophone located in an area where there may be many interfering noise sources, such as from moving ships, it is probably better to determine NRRL from  $S_{\text{OUT}}$  and  $N_{\text{OUT}}$  than from  $\left(\frac{S}{N}\right)_{\text{OUT}}$ . Thus, from Eqs. (24) and (25), we obtain

$$\text{NRRL} = \frac{1}{2} (S_{\text{OUT}} - N_{\text{OUT}}) + PL_{\text{MIN}} - 199.5, \text{ dB} \tag{27}$$

In the standard ocean the long range minimum propagation loss is approximately given by

$$\begin{aligned}
PL_{\text{MIN}} &= 10 \log 5.8 \text{ nm} + 10 \log R \text{ nm} + 20 \log 2000 \text{ yd/nm} \\
&= 73.7 + 10 \log R \text{ nm}, \text{ dB}
\end{aligned} \tag{28}$$

At  $R = 2000 \text{ nm}$ ,  $PL_{\text{MIN}} = 106.7 \text{ dB}$ . Therefore, at a range of 2000 nm in the standard ocean, the minimum detectable value of NRRL using Eqs. (25), (26) and (27) is equal to -89.8 dB.

As an illustrative example, assume that a signal has been received in the standard ocean environment. Let the output level of the signal,  $S_{\text{OUT}}$ , be

87 dB above the output level of the ambient noise before the signal arrives, and let the minimum propagation loss at a range of 1700 nm be 106 dB. Then, solving Eq. (27),  $NRRL = -50$  dB. This value of  $NRRL$  can now be used in Figure 6 to determine possible values of yield/altitude for an air nuclear detonation. For example, a 1-kiloton yield would be at an altitude of about 100 ft, a 10-kiloton yield at about 450 ft, and a 100-kiloton yield at about 1500 ft. This could not have been an underwater nuclear detonation because  $NRRL$  is too small.

After the detection of a nuclear detonation has been made, it might be desirable to perform a spectral analysis of the received signal in order to determine whether the higher critical frequency is below, within or above the 10 to 30 Hz passband. A 1-Hz narrowband resolution and an averaging time of 15 seconds are probably suitable for obtaining the signal spectrum. If this spectrum has a slope of  $-6$  to  $-3$  dB/octave, the critical frequency is below the passband and no correction to  $NRRL$  due to spectrum shape is required. If this spectrum has a slope of  $-3$  to  $+6$  dB/octave,  $NRRL$  is too low and should be corrected to a higher value. The amount of this correction is not large if the spectrum slope is less than 0 dB/octave, but if it is greater than 0 dB/octave the correction is likely to be significant. However, only low yield, low altitude nuclear detonations in the air will have a positive spectrum slope. This is the yield/altitude region which is subject to large  $NRRL$  errors due to other effects. It is also unlikely that such low yield air detonations will be tested and detected. Therefore, it is probably not necessary to provide corrections to  $NRRL$  due to spectrum shape.

### 2.3 Error Analysis

The passband filtered, detected and averaged output of the autocorrelation processor for the receiver hydrophone provides the basic measurements that are used to obtain yield-vs-depth/altitude estimates. These measurements are the processor output level, in dB, due to the received acoustic energy from a nuclear detonation ( $S_{OUT}$ ) and the output level due to ambient noise just before the arrival of the signal ( $N_{OUT}$ ). The dB difference in these two measurements ( $S_{OUT} - N_{OUT}$ ) can be obtained quite accurately, provided the hydrophone and processor are linear over the dynamic range of the signal. This dynamic range should be of the order of 60 dB for air bursts or underwater detonations, and about 120 dB for both. Such a large dynamic range requires an accurate automatic gain control (AGC) for the hydrophone receiver output, from which the full dynamic range of the signal can be linearly reconstructed. The standard deviation error in the measurement of ( $S_{OUT} - N_{OUT}$ ) is approximately 3.5 dB if the receiver system is linear but not calibrated. About 2.5 dB of this error may be due to an inaccurate estimate of the ambient noise level. If the receiver system is calibrated, this source of error can be eliminated, which reduces the estimated  $S_{OUT}$  measurement error to about 2.5 dB. With a calibrated system, Eq. (24), which does not require a measurement of  $N_{OUT}$  to determine NRRL, can be used. The other source of error in the estimation of NRRL is that due to error in the propagation loss (PL) calculation, which is estimated to be about 2 dB for ocean environments that approximate that of the assumed standard ocean. For other types of environments, the propagation loss error will probably be greater. Thus, the standard deviation error in NRRL is estimated to be about 3.2 dB using Eq. (24), and 4 dB using Eq. (27).

depending upon whether or not the receiver system is calibrated, for ocean environments that provide good long range propagation.

The calculation of NRRL does not provide a solution of the yield and depth/altitude of a nuclear detonation. It simply reduces the total set of yield-depth/altitude pairs to those which produce the same amount of acoustic energy as that actually received within the passband at long range. For an underwater nuclear detonation, the yield can be determined with fair accuracy even if the depth of the detonation is unknown. This is due to the fact that NRRL for a given yield varies a maximum of about 6.5 dB with depth. However, for an air burst, NRRL can vary by as much as 75 dB as a function of altitude (from 0 to 5000 feet) for a given yield. It was convenient to divide yield/altitude as a function of NRRL into two regions - that for which the detonation altitudes exceed the hydrodynamic separation range (Figure 6), and that for which the fireball interacts with the water before hydrodynamic separation (Figure 10). It can be seen from these figures that the possible yield-altitude pairs for a given value of NRRL - a vertical line - are simply those which intersect this line. Then, if by some other means, the value of altitude (or yield) can be obtained, the value of yield (or altitude) can also be obtained at the point on the vertical line where it intersects the altitude (or yield) line. An exception to this statement can be seen in Figure 6, where, for some values of NRRL and yield, the altitude is multivalued. For example, at  $\text{NRRL} = -50$  dB and yield (W) = 1 kiloton, the altitude may be either 15 feet or 90 feet.

Now, if the error statistics associated with NRRL are known, confidence limits on yield-vs-altitude determination can be specified. Values within these limits will fall within an area about the vertical line at the mean value of NRRL. If the NRRL error is a Gaussian distributed random variable

with a standard deviation of 4 dB, the probability that the true yield-altitude pairings fall within the vertical lines at 4 dB on either side of the mean value of NRRL is 0.68, and the probability that they fall outside these lines is 0.32. Thus, if the value of altitude (or yield) can be determined by some other means, the value of yield (or altitude) will have a random error that is a non-linear function of both the NRRL error and the altitude (or yield) error. An inspection of Figures 6 and 10 will show the variability of yield error as a function of NRRL and altitude - called  $Z_0$  in this discussion - for given values of error in each. For example, let NRRL in Figure 6 be -50 dB with a standard deviation error of 4 dB, and let  $Z_0$  be 1500 feet with zero error. Then, there is a 50-percent probability that the yield will be between 69 and 145 kilotons, and a 90-percent probability that it will be between 40 and 248 kilotons. (This assumes that the NRRL error is a Gaussian random variable with zero mean.) Next, let NRRL be -50 dB with zero error, and let  $Z_0$  be 1500 feet with a standard deviation error of 300 feet. If this altitude error is a Gaussian distributed random variable with zero mean, there is a 50-percent probability that the yield will be between 78 and 135 kilotons, and a 90-percent probability that the yield will be between 55 and 208 kilotons.

Looking at another region of yield-altitude as a function of NRRL, let NRRL in Figure 10 be -30 dB with a standard deviation error of 4 dB, and let  $Z_0$  be 28 feet with zero error. Then, there is a 50-percent probability that the yield will be between 9.7 and 10.4 kilotons, and a 90-percent probability that the yield will be between 9.2 and 10.9 kilotons. Now, let NRRL be -30 dB with zero error, and let  $Z_0$  be 28 feet with a standard deviation error of 6 feet. For this error in altitude there is a 50-percent probability that the yield will be between 7.7 and 13.8 kilotons, and a 90-percent probability that

the yield will be between 5.3 and 22.1 kilotons. These examples show the variability of the error in yield as a function of error in NRRL and as a function of error in altitude for different regions of altitude-NRRL space.

Another possible source of error in yield-altitude as a function of NRRL is the accuracy in the derivation and generation of the curves in Figures 6 and 10. All known variables were accounted for to first order, but some have been extrapolated to the extent that second order effects may introduce several dB of error in the acoustic energy levels in some regions of the yield-altitude space. Nevertheless, it is believed that these curves are as accurate as can be reasonably expected from theory and the available experimental data.

### 3. SUMMARY

A computational scheme is developed for the determination of yield vs depth/altitude based on a received underwater detonation-like acoustic signal in the deep ocean. Based on the phenomenology of nuclear detonations both underwater and in the atmosphere, the depth/altitude axis is divided into four regions: (a) underwater (detonation depth  $> 21W^{1/3}$  feet), (b) atmospheric (detonation altitude  $> 15W^{1/3}$  feet), (c) near-surface in air (detonation altitude  $< 15W^{1/3}$  feet), and (d) near-surface underwater (detonation depth  $< 21W^{1/3}$  feet).

For the underwater case, the determination of yield vs depth requires the employment of one (or more) of the extant Navy-approved propagation prediction models. Predictions are made for the detonation site-to-receiver great circle path for assumed source placements throughout the water column. Yield determinations are made based on the predicted propagation loss values and the known received signal.

Determination of yield vs altitude for the atmospheric case is based on a family of thirty-six normalized relative received level (NRRL) curves obtained for the subject environment. This curve set is obtained by the application of a simple scaling procedure to a corresponding permanently stored set of NRRL curves derived for a standard ocean/atmosphere construct. This scaling involves knowledge of the maximum inclination angle at the ocean surface - in the vicinity of the source - associated with the long range propagation modes ( $\theta_s$ ), and the maximum inclination angle at the depth of minimum source-to-receiver propagation loss (reference depth) associated with the long range modes ( $\theta_{sc}$ ) - also in the vicinity of the source. Scaling is made possible



by the strong  $\theta_s^3$  dependency exhibited in the equation for determination of relative received level (RRL). The classification system employs an indirect method for determination of  $\theta_s$  and  $\theta_{sc}$  based on the predicted source-to-receiver propagation loss for both a surface source (no upgoing energy) and a source located at the reference depth. The method makes the assumption of cylindrical spreading of the shot-generated acoustic energy in the vicinity of the receiver. The yield-vs-altitude curve for the atmospheric case is defined by the yield/altitude pairings within the NRRL curve family for which the value of NRRL is that computed for the reference depth yield.

As for the atmospheric case, the method for determination of yield vs altitude in the near-surface region is based on a set of permanently stored NRRL curves. In the near-surface region NRRL is assumed to be environmentally independent. The method used for determining yield vs altitude using the near-surface NRRL curves is identical to that employed for the atmospheric case.

In the near-surface underwater region, yield vs depth is determined by simple linear interpolation between the yield computed for the shallowest point on the underwater yield-vs-depth curve and that computed for a source located right at the surface.

The determination of NRRL for the reference depth is based on the passband filtered, detected and averaged output of an autocorrelation processor for the receiving hydrophone. The required measurements are the processor output level due to the received acoustic signal energy ( $S_{OUT}$ ) and the output level due to the ambient noise energy just before reception of the shot-generated signal ( $N_{OUT}$ ). The signal processing analysis is based on the assumption that within the operational frequency passband of the receiver (10 to 30 Hz) the spectrum slope of the detonation signal is -6 dB/octave.

This assumption is believed to be valid for most yield/altitude combinations for which detections can be made. Based on an averaging time of 15 s and a detection index of 23 dB, it is estimated that, for the 10 to 30 kHz band, the minimum detectable NRRL at a range of 2000 nm in the standard environment is about -90 dB. Due to the large dynamic range required by the system (~120 dB) an accurate automatic gain control (AGC) must be at the receiving sensor output. The standard deviation of the error in reference-depth NRRL determination is estimated to be about 3 dB for a calibrated linear receiving system and about 4 dB for an uncalibrated system.

For an air detonation the determination of yield (or altitude) requires that shot altitude (or yield) be determined by some other means. The error in determination will have a random error that is a nonlinear function of the error in NRRL and the error in altitude (or yield). For an underwater detonation, a determination of yield can be made with a relatively high accuracy - even if the depth is not known - because of the small variation in NRRL over the water column.

Other possible sources of error in the determination of yield vs altitude are those arising from inaccuracies in the derivation of the curves for the standard ocean/atmosphere, and from inaccuracies in the indirect method employed for determination of the angles used in scaling to subject environments. These have not been addressed in this project.

#### 4. RECOMMENDATIONS

The algorithmic design of a system for the detection, localization and classification of a possible nuclear detonation in the open ocean has been described in this Phase I report. It is recommended that a Phase II effort be undertaken for the software implementation of the four different yield-versus-depth/altitude algorithms (underwater, atmospheric, near-surface in-air, and near-surface underwater), and their integration with existing detection and localization software into a complete computer program. Any additional software development needed by the facility responsible for using this system, such as broadband and narrowband signal processors and localization techniques using time delays between direct arrivals and reverberant returns from such ocean features as continental slopes, seamounts and island chains is also recommended for Phase II.

The validity of the physical model used to obtain the atmospheric yield and altitude functional dependencies upon NRRL has not been fully confirmed experimentally. The derivation is based upon the use of the shock wave overpressure instead of the ambient pressure in calculating the speed of sound and density in air at the air-water boundary, and the employment of these values in linear acoustic equations. Qualitative comparisons based upon nuclear detonations and observations from very low yield chemical explosive experiments tend to support this physical assumption. We believe this model to be valid. If the shock overpressure assumption is correct, there will exist a lateral wave whenever the overpressure is sufficiently large that the speed of sound in air is greater than the speed of sound in water at the air-water boundary. Scale model chemical explosive experiments in air can be used to determine whether or not a lateral wave exists. It is recommended

that these tests be conducted in order to validate the physical basis for the yield-vs-altitude curves that have been derived. These tests need not impact on, nor be a part of the Phase II effort since the yield-vs-altitude curves can be easily modified due to any subsequent refinements in the physical theory.

Implementation of this system will improve the overall capability of the Federal Government to more quickly and accurately determine whether or not an at-sea detonation has occurred and to determine its location and yield-vs-depth/altitude curve. This will provide a greater opportunity for an aircraft to be dispatched to the site and collect radioactive air-borne particles before they have become too dispersed to be detected.

Implementation will require propagation loss models, environmental data banks and localization algorithms, all of which reside at NORDA. It is anticipated that the integrated system will be developed and implemented by working closely with NORDA personnel who are familiar with the software implementation of these models, data banks and algorithms. The completed system will reside at NORDA so that a quick response can be achieved for any suspected at-sea nuclear detection.

## APPENDIX A

### DETONATION LOCALIZATION

#### A.1 Background

Since 1973, the Navy, under the auspices of the Defense Nuclear Agency (DNA), has been heavily engaged in the study of the characteristics of ocean basin reverberation generated by large underwater detonations. The overall purpose of the effort is the determination of the potential impact of underwater nuclear detonations on the performance of underwater acoustic detection systems. The work has included theoretical studies, reverberation model development for prediction of pressure-time histories, model validation studies involving comparison of model predictions with actual data, and the planning and performance of field experiments involving the detonation of large chemical charges in the open ocean. Two computer-implemented reverberation prediction models have been developed and validated during this program - one by the Naval Surface Weapons Center (NSWC) and the other by Underwater Systems, Inc. (USI), (as of 1 March 1984, Underwater Systems, Inc. has become Underwater Systems Group (USG), a division of Mandex, Inc). The major results of the reverberation program are reported in References 4 to 6.

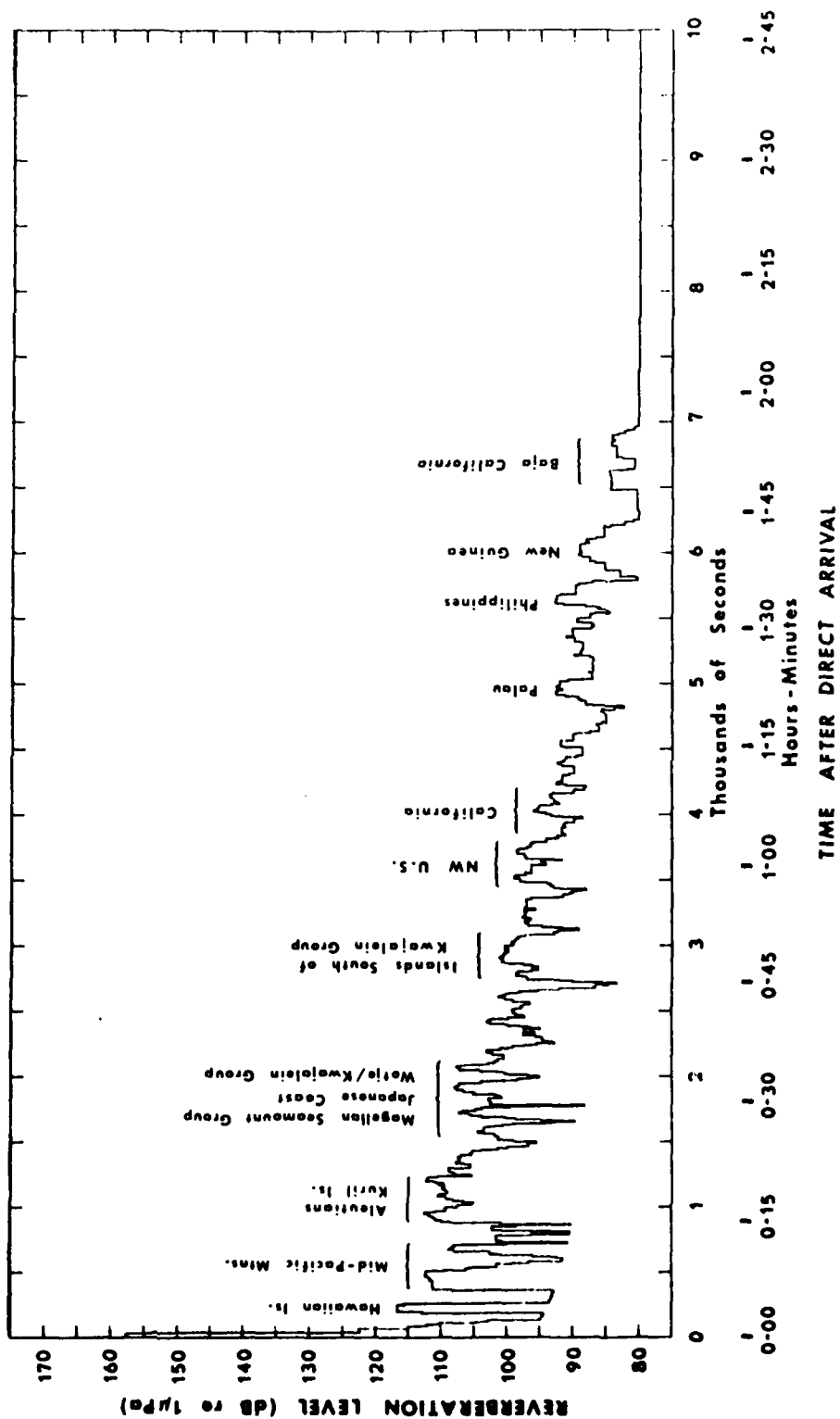
Additional investigations and analyses have been performed addressing the question of the feasibility of determining the location, yield and depth of an underwater nuclear blast through analysis of the reverberant returns at a single underwater sensor, Reference 7. The results of this work have been quite encouraging.

#### A.2 Source Location Determination

In general, ocean basin reverberation generated by underwater detonations can be characterized as comprising three basic components: (1) a direct signal

of very high amplitude arriving via the great circle track connecting the source and receiver; (2) intermittent large-amplitude scattered returns from prominent basin reflectors such as continental slopes, island chains and seamounts; and, (3) lower level reverberation caused by scattering at the ocean surface and basin bottom as well as by multiple reflections from the basin walls. The reverberation pressure-time history (levels, duration and envelope shape) at any given site is a strong function of source level, source and receiver locations within the basin, and the basin geometry. Figure A-1, taken from Reference 6, shows an example of a predicted 100 Hz pressure-time history for a hypothetical underwater 1-megaton detonation located in the North Pacific Ocean. The source and receiver locations are specified on the figure. Also identified are the basin reflectors associated with many of the discrete returns. The ambient 100 Hz noise level was taken as 80 dB// $\mu$ Pa/Hz. Note that for this case reverberant signals of significant level are predicted up to nearly two hours after the reception of the direct arrival.

It is the presence of the intermittent returns in large charge reverberation time histories which afford the opportunity for estimation of shot location. Consider the illustration shown as Figure A-2. The figure depicts the direct arrival propagation track and the propagation track associated with the scattered returns from a single prominent basin reflector, or, "hot spot." The reverberation track comprises two legs - the propagation path from the source to the reflector and the path from the reflector to the receiver. The ranges associated with the direct arrival track and the first and second legs of the reverberation track are given as  $R_D$ ,  $R_{S,HS}$  and  $R_{HS,R}$ , respectively. If we assume some representative sound speed ( $c$ ) for the basin, the elapsed time after the direct signal ( $\Delta T$ ) at which the reverberation return arrives at the receiver is given by



Source: 40-00N, 160-00E

Receiver: 21-49N, 157-56W

Figure A-1. 100 Hz Reverberation for a Hypothetical 1-Megaton Detonation in the North Pacific Ocean.

From Reference 6.

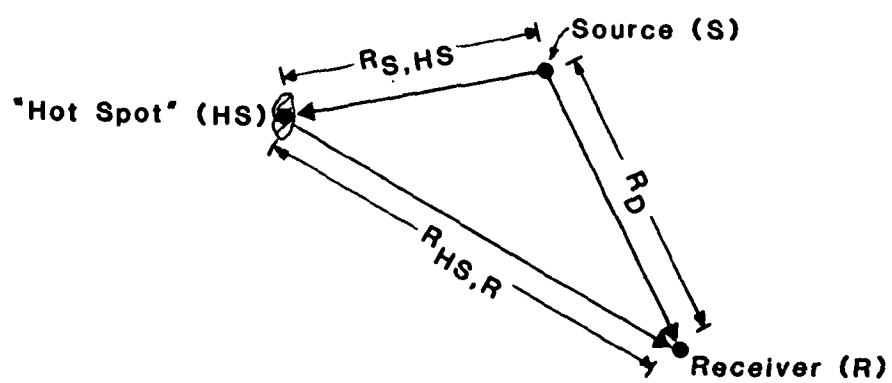


Figure A-2. Geometry Associated with Reverberant Return from a Basin Reflector ("Hot Spot"). (See text.)



$$\Delta T = \frac{1}{C} (R_{S,HS} + R_{HS,R} - R_D) \quad (A-1)$$

Assume, now, that a reverberation time history has been obtained for an underwater event and that the location of the detonation is unknown. Also, assume that, based on previous knowledge of the reverberation characteristics of the basin (obtained, say, by field experimentation or model predictions) that a number of basin "hot spots", have been determined to be associated with specific peaks in the history. For each "hot spot", then,  $\Delta T$  and  $R_{HS,R}$  are known. For each case the locus of points of source locations which satisfy Eq. (A-1) can now be determined. Neglecting all error, the resulting curves will intersect at the true source location. In actual practice, various timing errors will result in curve crossings over some finite area in the vicinity of the source. The nominal location is taken as some centrally located point within the region of uncertainty. The proper identification of "hot spots" with specific reverberant returns is, of course, crucial to the method. Once an estimate of a detonation site location has been made, the location can be tested by making a time-history prediction for the site using one of the extant reverberation prediction models and comparing the results with the measured history.

### A.3 Reverberation Models

(NOTE: With minor modification, the following discussion was taken directly from Reference 4.)

Two computer models for predicting ocean basin reverberation have been developed and continually refined over the past several years. One model was developed by NSWC and the other was developed by USI under contract to NSWC. Both models were initially developed to predict reverberation in the North

Atlantic Basin. Experimental measurements had been made in that area, and the data could be used for validation purposes. Both models approach the prediction of reverberation in a similar manner, but with some essential differences. The NSWC model is designed more for quantity production, so simplifying assumptions have been made to reduce computer running time. The USI model is basically a research tool used to investigate special aspects of reverberation in a basin. A brief discussion of each model follows.

#### A.3.1 NSWC Reverberation Model

The Naval Surface Weapons Center model is based on the following assumptions and procedures:

- a. Sound travels over long distances via the sound channel along great circle paths.
- b. The basin boundary is defined by an appropriate depth contour. For the North Atlantic and North Pacific, a depth of 1000 fathoms has been used.
- c. Individual reflectors in the basin, such as islands or seamounts, are defined at the same depth as the basin boundary.
- d. Sound energy spreads spherically to a range of 10 nm from the source (or reflector), and cylindrically thereafter.
- e. A modified Thorp equation is used to calculate the absorption in water.
- f. A constant scattering strength is assumed throughout the basin. The strength of each reflector is determined by multiplying this constant (determined empirically) by a function of slope angle.
- g. Individual signals are spread in time, 1 second for each 100 nm of travel, to account for multipath effects. In addition, they are spread to account for the size of the reflector.

- h. Surface reverberation is provided by the USI model.
- i. Multiple bounces off the basin walls may occur and can be treated.
- j. Modeling a single frequency is adequate to define the basin reverberation in the 10 to 250 Hz band. It has been determined experimentally that only absorption corrections need be applied to determine the reverberation at other frequencies within the band.

Making use of these assumptions and procedures, the model calculates a reverberation record in a straightforward manner.

Figure A-3 shows a simple basin model. The continental boundary and obstructions within are defined by the open circles and the great circle segments which connect them. Each segment that connects open circles is considered a reflector. Boundary points which are not connected define non-reflecting or open segments. The source and receiver are designated by the points marked S and R.

With the geometry defined, the computer model checks all possible paths from the source to the receiver. Of the sample paths shown, the direct path (1) and a single-bounce path (5) reach the receiver. If desired, double- and triple-bounce paths\* are also computed. For each path that reaches the receiver, signal amplitude, travel time and duration are computed.

A reverberation record is generated by energy summing all the individual arrivals in 10-second bins. These discrete arrivals are added to the surface reverberation (calculated from the USI model) and the ambient noise.

---

\*A double-bounce path is one that interacts with two boundary segments before reaching the receiver; a triple-bounce path interacts with three boundary segments.

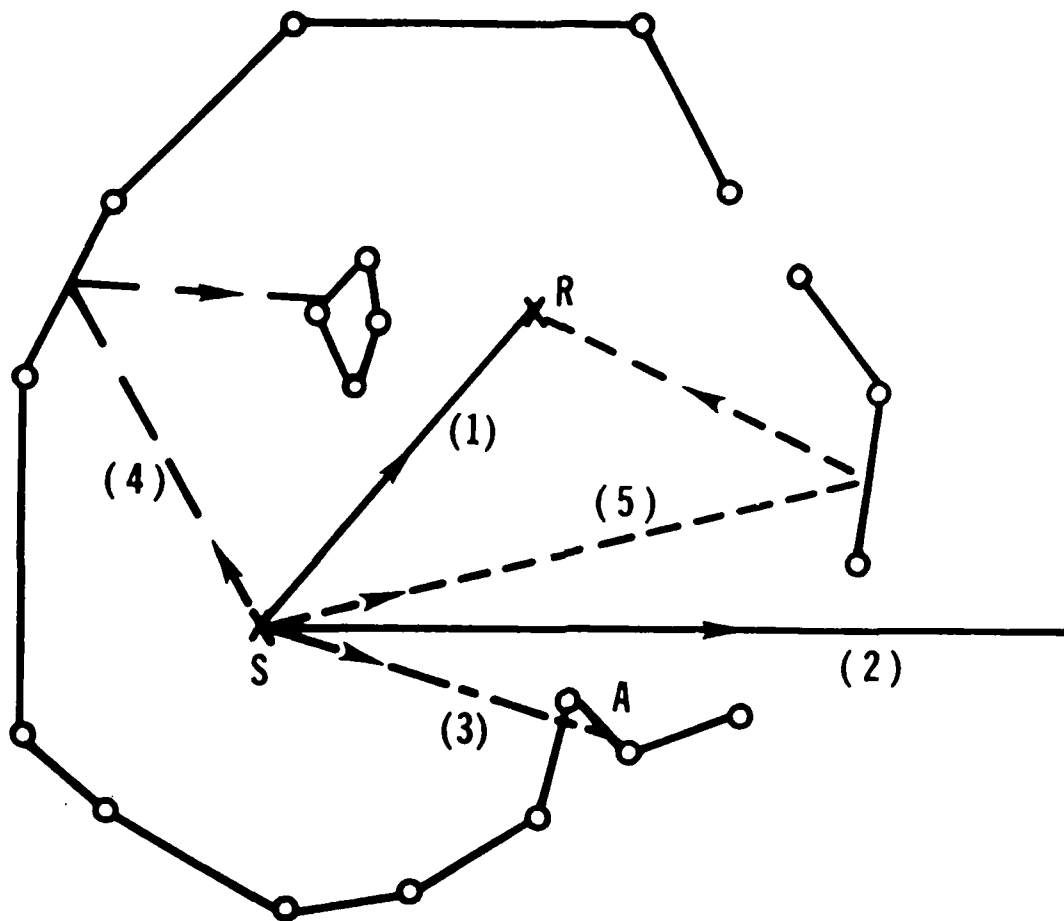


Figure A-3. Simple Basin Model Showing Various Types of Paths from the Source.

### A.3.2 USI Reverberation Model

The USI reverberation model was developed concurrently with the NSWC model. The model treats surface reverberation and boundary or seamount reflections with attenuation as a function of grazing angle. Multiple boundary bounces, however, cannot be accommodated.

The reverberation level due to sea surface reverberation is based on the following equation:

$$RL_s = SL + SS + 10 \log A - PL_1 - PL_2 - \alpha(R_1 + R_2) \quad (A-2)$$

where

$RL_s$  is the surface reverberation level in dB// $\mu$ Pa/Hz

$SL$  is the source level in dB// $\mu$ Pa/Hz

$SS$  is the scattering strength of the surface in dB

$A$  is the ensonified surface area

$PL_1$  is the spreading loss, in dB, from the source to the surface area  
( $1/R^2$  to 10 nm, then  $1/R$ )

$PL_2$  is the spreading loss, in dB, from the surface area to the receiver

$\alpha$  is the absorption coefficient

Figure A-4 shows the geometry associated with the implementation of Eq. (A-2). The elliptical ring depicts the area on the surface from which scattered sound arrives at the receiver if a one second pulse width is assumed. The source (S) and the receiver (R) are at the foci of the ellipse. Calculations are made by dividing the elliptical ring into  $n$  increments of angular width  $\Delta\theta_n$  with each annular section having an incremental area  $\Delta A_n$ . The scattered energy from each  $\Delta A_n$  is then integrated over the entire ring.

Surface reverberation versus time is calculated by repeating this process for each second of time in ever-growing elliptical rings. When the elliptical ring crosses a boundary segment, the angular increment subtended by the

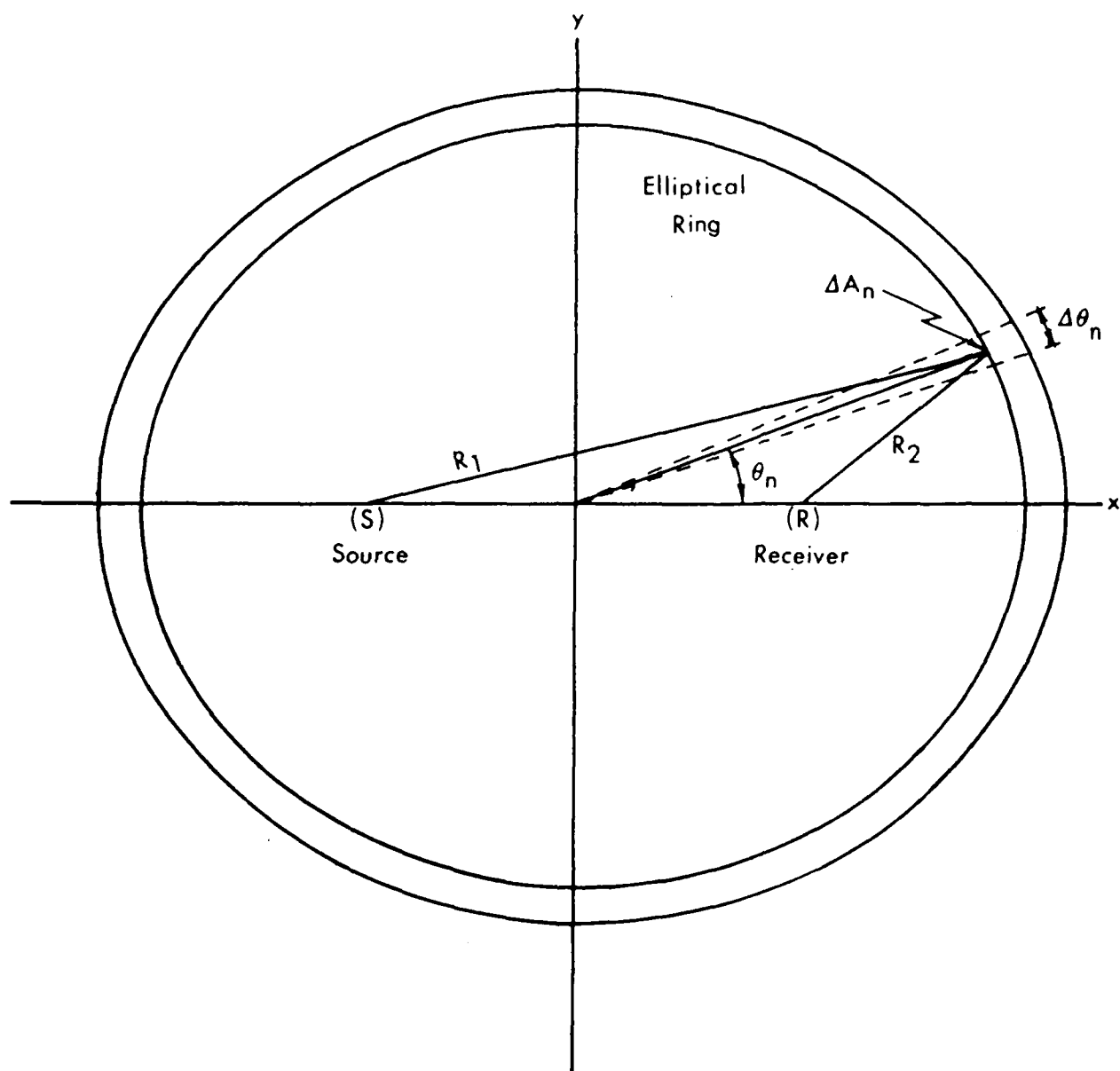


Figure A-4. Geometry for the Sea-Surface Reverberation Calculation as Viewed from Above the Surface.

boundary segment is excluded from the total surface reverberation level of that and all subsequent elliptical rings. The calculations continue until the ellipse has crossed all boundary segments, or 2 hours after the direct arrival.

In the coastal reverberation part of this model, a sloping continental shelf is described by a series of straight line segments from which multiple-bounce reverberation occurs, as illustrated in Figure A-5. For each coastal segment, a ray analysis is used to determine the angle and depth of the incident ray. Using appropriate bottom loss- and bottom backscattering-versus grazing-angle values, sets of reverberation strengths and reverberation times are calculated for the bottom encounters depicted in Figure A-5. The times are calculated relative to the first bottom bounce. When a range of incident angles and depths is possible, the reverberation strengths and times used are an average of the possible values.

The reverberant energy from each bottom encounter is distributed evenly over a time interval appropriate to the size of the boundary segment. The ranges from the source to the first encounter ( $R_1$ ) and from the first encounter to the receiver ( $R_2$ ) are used to determine spreading loss and attenuation for the set of bottom encounters. The ambient noise level is added to the computed reverberation levels.

The total reverberation record is constructed by energy summing the coastal reverberation levels from all of the boundary segments with the surface reverberation levels previously calculated, integrated over 10-second intervals.

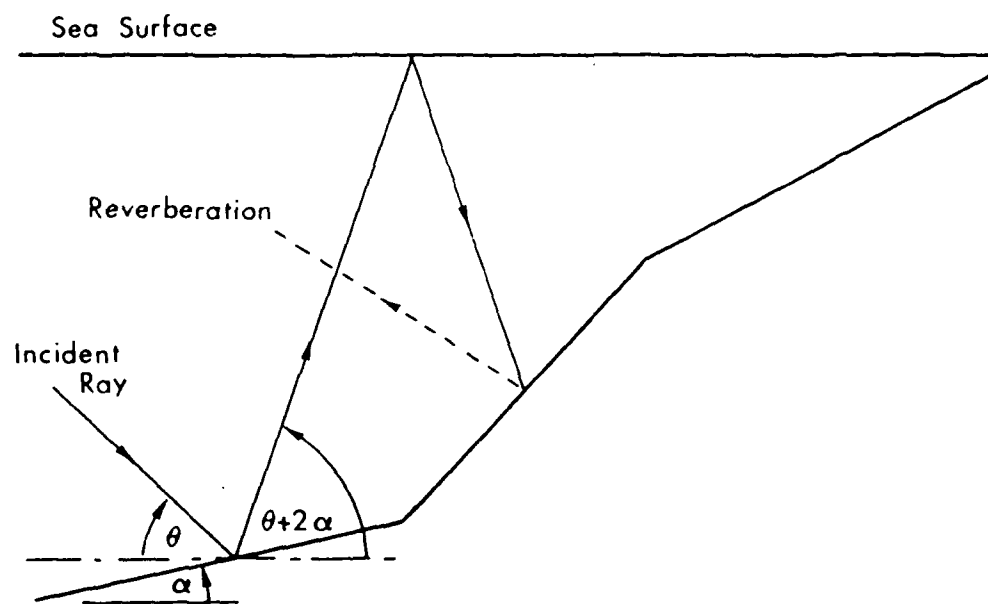


Figure A-5. Coastal Reverberation Model - Upslope Propaga



## APPENDIX B

### SEISMIC SIGNALS

The efficiency with which underwater detonations generate seismic signals detectable at teleseismic ranges is well established (References 8 and 9).

One would expect that atmospheric detonations over the ocean would have a very low efficiency of seismic excitation.

A first estimate of the reduction in energy available for seismic excitation can be obtained by considering the downward refraction of energy as given by the equations of Reference 10. This loss is given by:

$$L = 10 \log \left[ \frac{(\rho_1 c_1 + \rho c)^2}{4 \rho c \rho_1 c_1} \frac{c_1^2}{c^2} \right] \text{ decibels} \quad (\text{B-1})$$

where

$$\rho = \rho_0 \left( \frac{7 + 6p/P_0}{7 + p/P_0} \right) \quad (\text{B-2})$$

where

$\rho$  is the density of air behind the shock front at the air-water interface

$\rho_0$  is the ambient density

$p$  is the peak overpressure (behind the shock front)

$P_0$  is the ambient pressure (ahead of the shock)

$$\rho_0 = 0.001253 \text{ g/cm}^3$$

$$P_0 = 14.7 \text{ psi}$$

$$c = c_0 \left( 1 + \frac{6p}{7P_0} \right)^{1/2} \quad (\text{B-3})$$

where

$c$  is the shock velocity in air at the air-water interface

$c_0$  is the ambient speed of sound (ahead of the shock front)  
 $p$  is the peak overpressure (behind the shock front)  
 $P_0$  is the ambient pressure (ahead of the shock)  
 $c_0 = 33528 \text{ cm/sec (1100 ft/sec)}$   
 $P_0 = 14.7 \text{ psi}$   
 $\rho_1$  is the density of water behind the shock front at the air-water interface  
 $c_1$  is the shock velocity in water at the air-water interface

These equations are consistent with what we have done in analyzing the acoustic problem. The shock wave velocity and density in air is used in linear acoustic equations which properly handle refraction and sphericity to predict the downward propagating signal. The results are shown in Figure B-1 which shows the loss as a function of altitude for parametric yields ranging from 0.01 kiloton to 10 megatons. Note that there is a yield-altitude region for which the value of  $L$  is negative. That is, there is a gain rather than a loss. This is caused by the downward refraction of the energy which is sufficient to overcome the impedance mismatch at high enough shock velocities.

The loss factor  $L$  describes only the loss of energy transmitted through the interface. As compared to an underwater detonation, there are additional losses. This includes 3 dB corresponding to the loss of the upward propagating energy (reflected from the sea surface) which exists for the underwater detonation, and about 6 dB corresponding to the loss of the bubble pulse energy which is a major contributor to the low frequencies considered in seismic signals. Taking these factors into

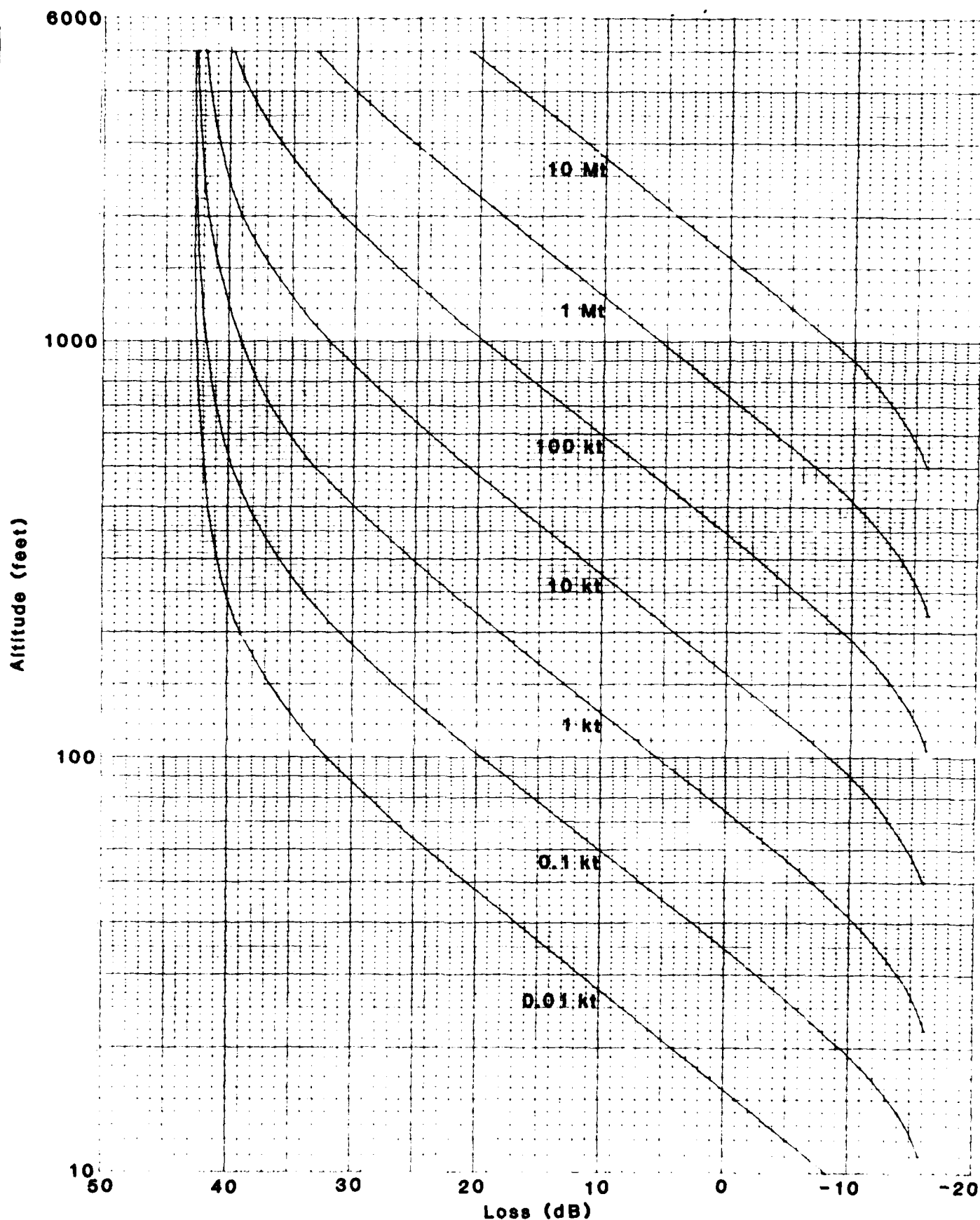


Figure B-1. Energy Loss Through the Air-Water Interface as a Function of Altitude for the Indicated Yields.

account, the results of Figure B-1 can be replotted as shown in Figure B-2.

The solid lines of Figure B-2 show the yield/altitude curves for fixed total excitation losses (parameterized). The dashed lines provide a means for relating deep underwater and atmospheric detonations. For example, a 200-kiloton atmospheric detonation at an altitude of about 240 feet will generate the same seismic signal as a deep underwater detonation of 250 kilotons. Similarly, a 20-kiloton detonation at an altitude of 110 feet is equivalent to a deep underwater detonation of about 25 kilotons.

The numerical values provided by Figure B-2 should not be taken too literally. Energy of atmospheric detonations is crudely modeled by  $10 \log W$  decibels, where  $W$  is the yield, and the upward going energy and bubble pulse of the underwater detonation are only crudely treated. Further, on fundamental considerations, we would expect that for a surface detonation the available energy would be reduced by 9 dB. The computations indicate that the efficiency of excitation is higher for the low altitude atmospheric detonations.

However, it is safe to conclude that low altitude nuclear detonations can generate detectable seismic signals comparable to those produced by underwater detonations. The parametric line designated by -1 dB (gain) roughly represents the yield/altitude curve above which the energy available for generating seismic signals reduces rapidly.

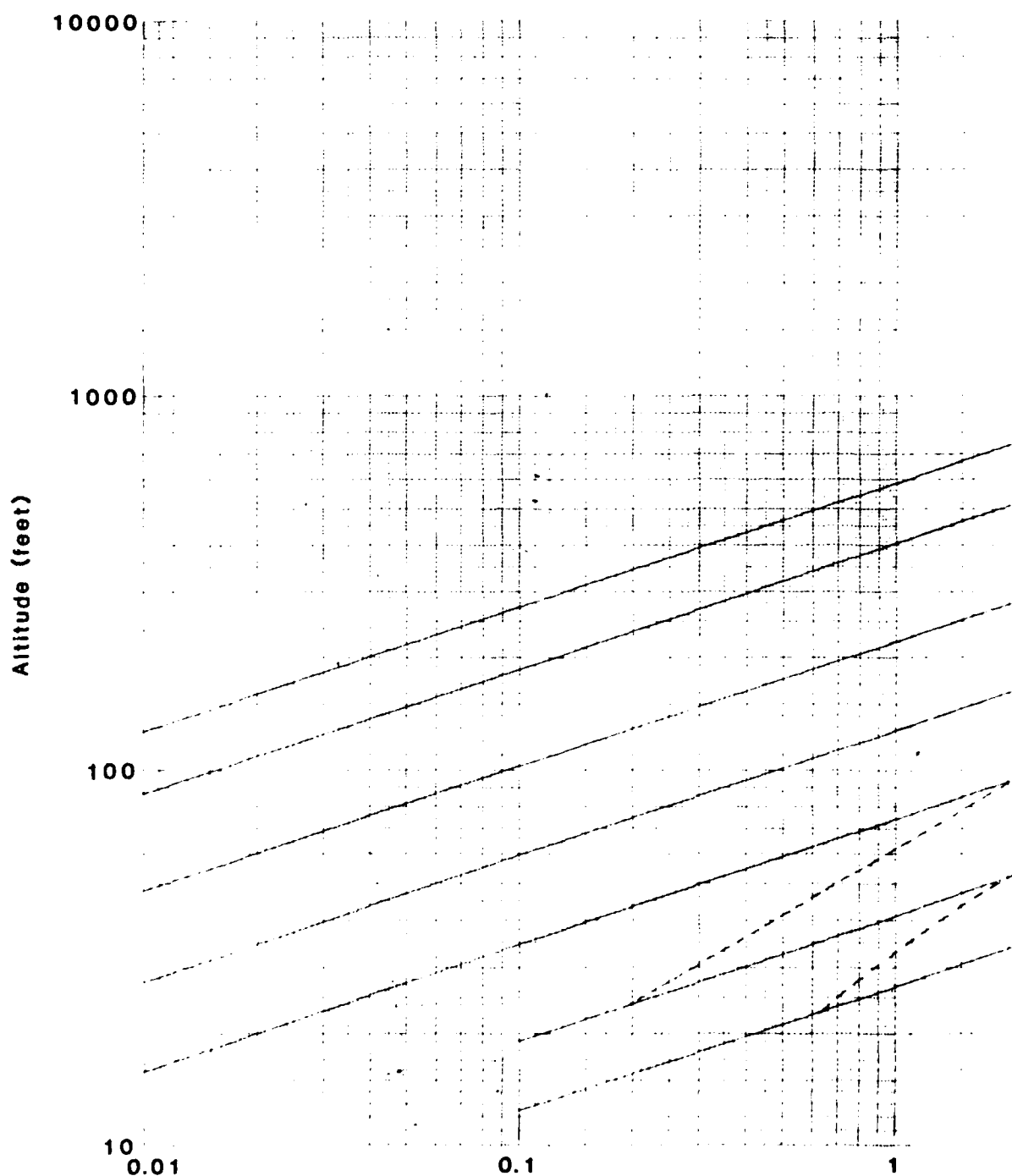
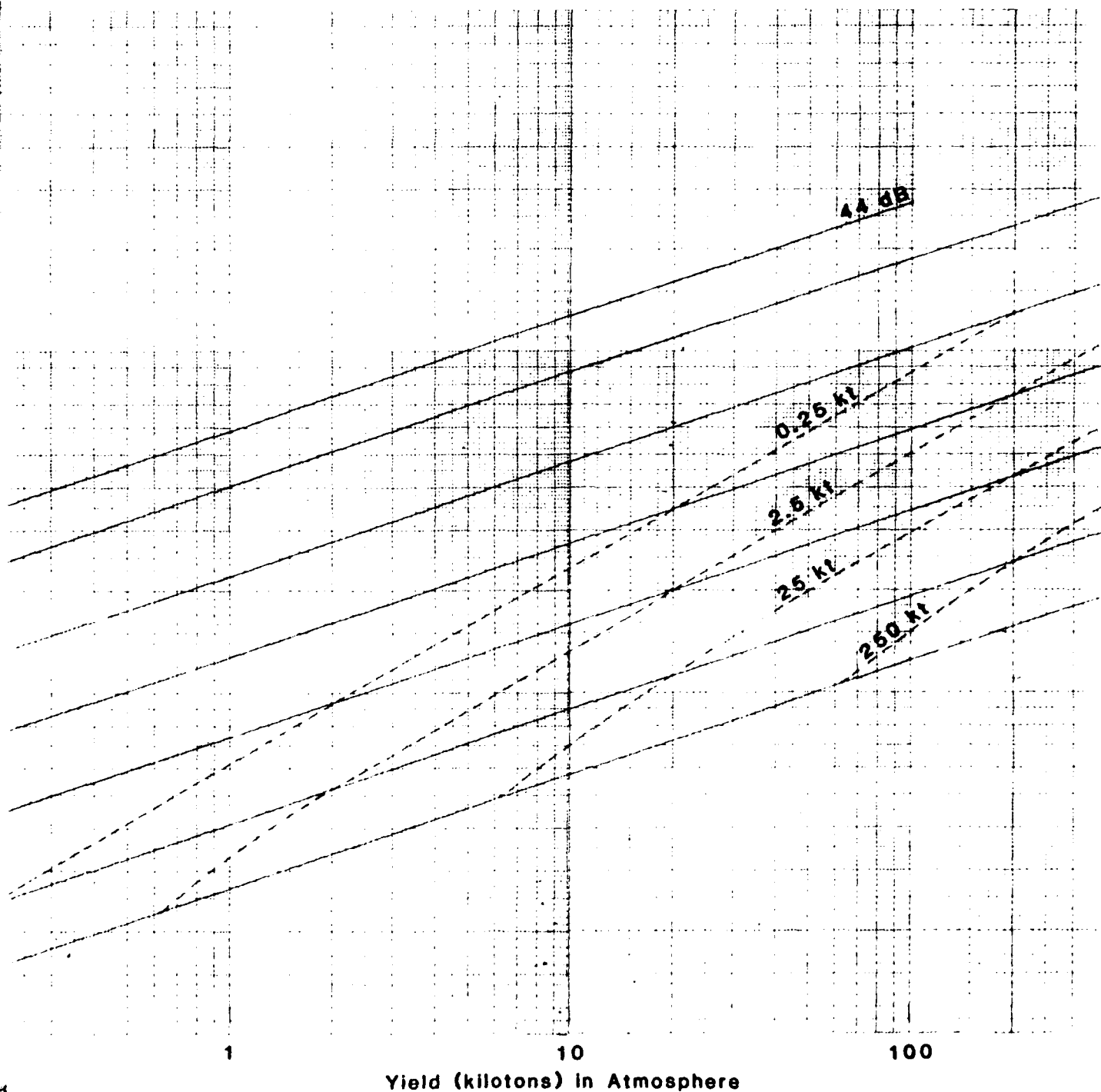


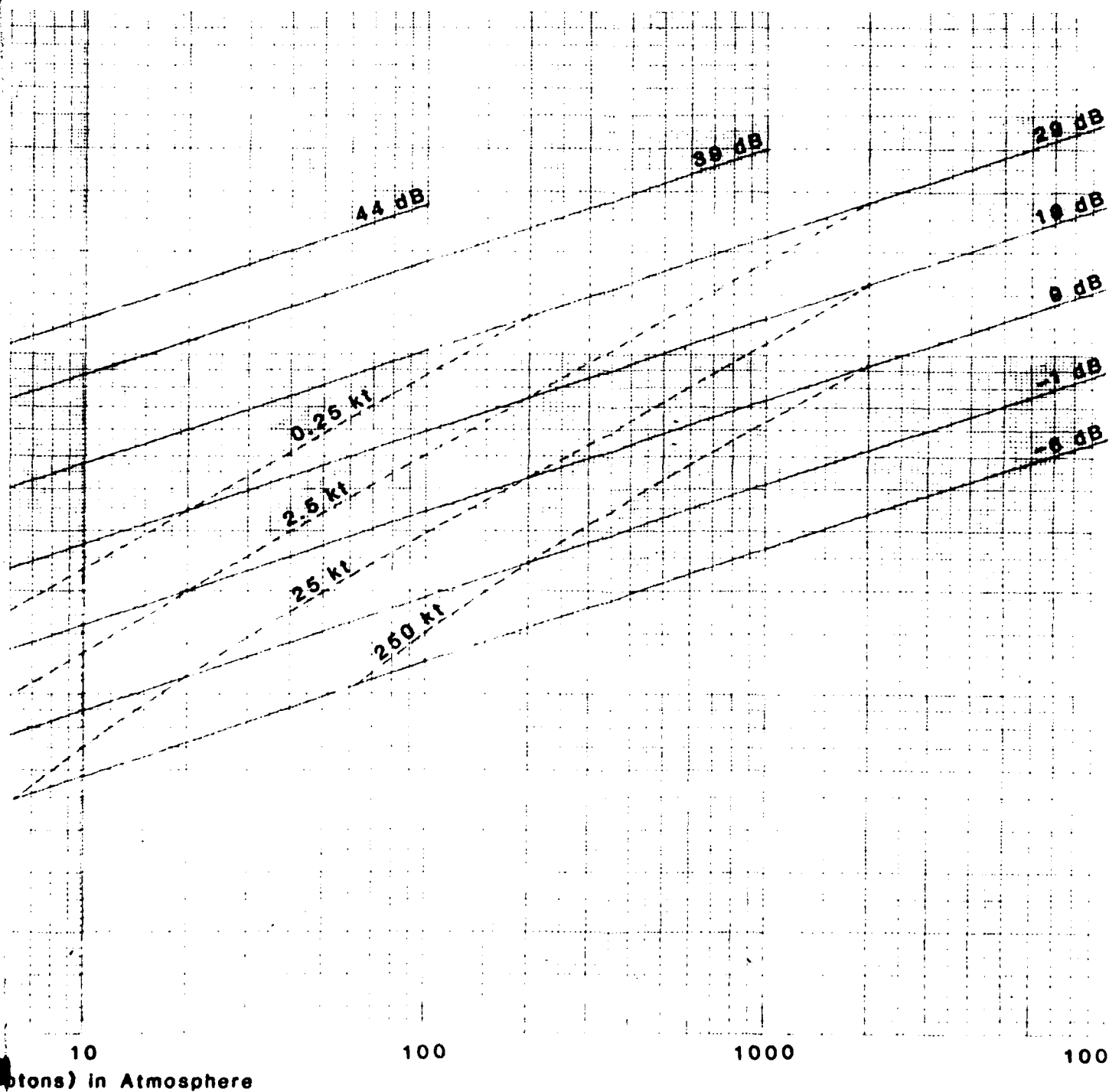
Figure B-2. Yield/Altitude Curve

(Dashed curves show yield/altitude  
be equivalent to those generated



3-2. Yield/Altitude Curves (Solid Lines) for Indicated Total Excitation Losses.

curves show yield/altitude points for which the seismic signals generated would be equivalent to those generated by the indicated underwater yields (parameterized.)



(lines) for Indicated Total Excitation Losses.

for which the seismic signals generated would  
indicated underwater yields (parameterized.)

## References

1. Weinstein, M. S. and E. L. Sander, "Underwater Signals Received at Long Range from Near Surface Nuclear Explosions," Underwater Systems, Inc., 6 January 1982.
2. Blatstein, I. M., "The Effect of Reverberation from Underwater Nuclear Explosions on Acoustic Detection Systems, Interim Report(U)," Naval Surface Weapons Center, White Oak Laboratory, NSWC/WOL/TR 76-82, 2 February 1977, Secret - Formerly Restricted Data.
3. Weinstein, M. S. and E. L. Sander, "Underwater Signals Received at Long Range from Near Surface Nuclear Explosions(U)," Underwater Systems, Inc., October 1982, Secret.
4. Hess, J. A., L. A. Mole and E. Tanglis, "Nuclear Reverberation Effects on Sonar Systems(U), Volume I - General Information(U)," Naval Surface Weapons Center, NSWC TR 80-61, 9 April 1981, Secret.
5. Hess, J. A., D. W. Dublin and E. Tanglis, "Nuclear Reverberation Effects on Sonar Systems, Volume II - North Atlantic Basin(U)," Naval Surface Weapons Center, NSWC TR 80-373, 15 August 1982, Confidential.
6. Wallace, W. E. and D. W. Dublin, "Nuclear Reverberation Effects on Sonar Systems(U), Volume III - North Pacific Ocean(U)," Underwater Systems, Inc., 12 September 1980, Confidential.
7. Weinstein, M. S., Letter Report - Analysis of Reverberation Tape - Contract No. N60921-79-C-0084(U), Underwater Systems, Inc., 17 April 1981, Secret.
8. Weinstein, M. S., "Spectra of Acoustic and Seismic Signals Generated by Underwater Explosions During Chase Experiment," J. Geophys. Res., Vol. 73, No. 16, 15 August 1968.
9. Evernden, J. F., "Magnitude Versus Yield of Explosions," J. Geophys. Res., Vol. 75, No. 5, 10 February 1970.
10. Hudimac, A. A., "Ray Theory Solution for the Sound Intensity in Water Due to a Point Source Above It," J. Acoust. Soc. Am., Vol. 29, No. 8, August 1957.



END

DATE  
FILMED

-84

DTIC

